Numerische Mathematik (2023) 154:369–408
https://doi.org/10.1007/s00211-023-01366-8

Numerische Mathematik

Stabilization-free HHO a posteriori error control

Fleurianne Bertrand[1] · **Carsten Carstensen**[2] · **Benedikt Gräßle**[2] · **Ngoc Tien Tran**[3]

Received: 3 July 2022 / Revised: 17 May 2023 / Accepted: 19 July 2023 /
Published online: 9 August 2023

Abstract
The known a posteriori error analysis of hybrid high-order methods treats the stabilization contribution as part of the error and as part of the error estimator for an efficient and reliable error control. This paper circumvents the stabilization contribution on simplicial meshes and arrives at a stabilization-free error analysis with an explicit residual-based a posteriori error estimator for adaptive mesh-refining as well as an equilibrium-based guaranteed upper error bound (GUB). Numerical evidence in a Poisson model problem supports that the GUB leads to realistic upper bounds for the displacement error in the piecewise energy norm. The adaptive mesh-refining algorithm associated to the explicit residual-based a posteriori error estimator recovers the optimal convergence rates in computational benchmarks.

Mathematics Subject Classification 65N12 · 65N30 · 65Y20

This work has been supported by the Deutsche Forschungsgemeinschaft (DFG) in the Priority Program 1748 *Reliable simulation techniques in solid mechanics. Development of non-standard discretization methods, mechanical and mathematical analysis* under the projects BE 6511/1-1 and CA 151/22-2 as well as the European Union's Horizon 2020 research and innovation programme (Grant Agreement No. 891734). The third author is also supported by the Berlin Mathematical School.

✉ Carsten Carstensen
cc@math.hu-berlin.de

Fleurianne Bertrand
fleurianne.bertrand@mathematik.tu-chemnitz.de

Benedikt Gräßle
graesslb@math.hu-berlin.de

Ngoc Tien Tran
ngoc.tien.tran@uni-jena.de

[1] Technische Universität Chemnitz, Chemnitz, Germany

[2] Humboldt-Universität zu Berlin, Berlin, Germany

[3] Friedrich-Schiller-Universität Jena, Jena, Germany

1 Introduction

Hybrid high-order methods (HHO) were introduced in [26, 27] and are examined in the textbooks [25, 29] as a promising class of flexible nonconforming discretization methods for partial differential equations that involve a parameter-free stabilization term for the link between the volume and skeletal variables.

1.1 Known a posteriori error estimator

The a priori error analysis of HHO involves the stability terms in extended norms as part of the methodology and motivated a first explicit residual-based a posteriori error estimator in [25] with a reformulation of the stabilization in the upper bound. Let $s_h(u_h, u_h)$ denote the stabilization at the discrete solution $u_h \in V_h$ and let the (elliptic) reconstruction Ru_h of u_h denote a piecewise polynomial of degree at most $k+1$ that approximates $u \in H^1(\Omega)$, cf. (2) and Sect. 3 below for further details. Then a possible error term reads

$$\text{total error}^2 := \|\nabla_{\text{pw}}(u - Ru_h)\|^2_{L^2(\Omega)} + s_h(u_h, u_h). \tag{1}$$

It is disputable if $s_h(u_h, u_h) \geq 0$ is an error contribution, but if the total error includes $s_h(u_h, u_h)$ (or an equivalent form), then the error estimator may also include this term (or a computable equivalent) for a reliable and efficient a posteriori error control. Amongst the many skeletal schemes like (nonconforming) virtual elements, hybridized (weak) discontinuous Galerkin schemes et al., the HHO methodology has a clear and efficacious stabilization

$$s_h(v_h, w_h) := \sum_{T\in\mathcal{T}} \sum_{F\in\mathcal{F}(T)} h_F^{-1} \langle S_{TF} v_h, S_{TF} w_h\rangle_{L^2(F)} \tag{2}$$

with the abbreviation $S_{TF} v_h := \Pi_{F,k}\left(v_{\mathcal{T}} + (1 - \Pi_{T,k})Rv_h\right)|_T - v_{\mathcal{F}}|_F$ for $v_h = (v_{\mathcal{T}}, v_{\mathcal{F}}) \in V_h$ in terms of the L^2 projections $\Pi_{K,k}$ onto polynomials of degree at most k on a facet or simplex $K \in \mathcal{F} \cup \mathcal{T}$ of diameter $h_K = \text{diam}(K)$; cf. Sect. 1.4 for further details. The original residual-based estimator η_{HHO} from the textbook [25] for the Poisson model problem $-\Delta u = f$ includes (2) and an interpolation $\mathcal{A}Ru_h \in V$ of Ru_h by nodal averaging in

$$\begin{aligned}\eta^2_{\text{HHO}} = {} & \|h_{\mathcal{T}}(1 - \Pi_0)(f + \Delta_{\text{pw}} Ru_h)\|^2_{L^2(\Omega)} + \|\nabla_{\text{pw}}(1 - \mathcal{A})Ru_h\|^2_{L^2(\Omega)} \\ & + s_h(u_h, u_h).\end{aligned}$$

(Multiplicative constants are undisplayed in this introduction for simplicity.) The results from Theorem 4.3 and 4.7 in [25] show reliability and efficiency for the total error (1) and piecewise polynomial source terms $f \in P_{k+1}(\mathcal{T})$,

$$\text{total error}^2 \approx \eta^2_{\text{HHO}}.$$

1.2 Stabilization-free a posteriori error control

There are objections against the double role of $s_h(u_h, u_h)$ on both sides of the efficiency and reliability estimate. First, the term $s_h(u, u_h)$ may dominate both sides of the error estimate. In other words, the total error might be equivalent to $s_h(u_h, u_h)$, but the quantity of interest may exclusively be

$$\text{error}^2 := \|\nabla_{\text{pw}}(u - Ru_h)\|^2_{L^2(\Omega)}.$$

Second, since the stabilization (2) incorporates a negative power of the mesh-size, a reduction property for local refinements remains unclear but is inevitable in the proofs of optimal convergence of an adaptive algorithm [5, 16]. This paper, therefore, asks a different question about the control of the error without the stabilization term (2) in the upper bound and introduces two stabilization-free error estimators (multiplicative constants are undisplayed)

$$\eta^2_{\text{res}} = \|h_{\mathcal{T}}(f + \Delta_{\text{pw}} Ru_h)\|^2_{L^2(\Omega)} + \sum_{F\in\mathcal{F}} h_F \|[\nabla_{\text{pw}} Ru_h]_F\|^2_{L^2(F)},$$
$$\eta^2_{\text{eq},p} = \text{osc}^2_{k+p}(f, \mathcal{T}) + \|Q_p - \nabla_{\text{pw}} Ru_h\|^2_{L^2(\Omega)} + \|\nabla_{\text{pw}}(1 - \mathcal{A}) Ru_h\|^2_{L^2(\Omega)}$$

for some parameter $p \in \mathbb{N}_0$. The explicit residual-based a posteriori error estimator η_{res} follows from the a posteriori methodology in the spirit of [14, 18, 20, 21] with a piecewise volume residual $f + \Delta_{\text{pw}} Ru_h$ and the jumps $[\nabla_{\text{pw}} Ru_h]_F$ across a facet F (on the boundary this is only the tangential component of $\nabla_{\text{pw}} Ru_h$). The equilibrated error estimator $\eta_{\text{eq},p}$ includes the post-processed quantity $Q_p \in RT_{k+p}(\mathcal{T})$ in the space $RT_{k+p}(\mathcal{T})$ of Raviart-Thomas functions of degree $k + p$ for $p \in \mathbb{N}_0$ and the nodal average $\mathcal{A}Ru_h \in S^{k+1}_0(\mathcal{T})$ of Ru_h. The main results establish reliability and efficiency

$$\text{error}^2 + \text{osc}^2_{k-1}(f, \mathcal{T}) \lesssim \eta^2_{\text{res}} \approx \eta^2_{\text{eq},p} \lesssim \text{error}^2 + \text{osc}^2_q(f, \mathcal{T})$$

for any $p, q \in \mathbb{N}_0$ up to data-oscillations $\text{osc}^2_q(f, \mathcal{T}) := \|h_{\mathcal{T}}(1 - \Pi_q) f\|^2_{L^2(\Omega)}$ of the source term $f \in L^2(\Omega)$ and without any stabilization terms. Computational benchmarks with adaptive mesh-refinement driven by any of these estimators provide numerical evidence for optimal convergence rates.

1.3 Further contributions and outline

The higher-order Crouzeix-Raviart finite element schemes are complicated at least in 3D [23] and then the HHO methodology is an attractive alternative even for simplicial triangulations with partly unexpected advantages like the computation of higher-order guaranteed eigenvalue bounds [15]. Higher convergence rates rely on an appropriate adaptive mesh-refining algorithm and hence stabilization-free a posteriori error estimators are of particular interest. The recent paper [36] establishes the latter for

Table 1 Explicit constants $C_1, C_{\mathrm{st}}, C_2$ for right-isosceles triangles with respect to the maximum interior angle $\omega_{\max}$ of the polygonal domain Ω

$\omega_{\max}$	π	$3\pi/2$	2π
M_{bd}	4	6	8
c_{apx}	2.9568	6.4642	11.3771
C_{st}	26.0893	55.8498	97.5374
C_1	2.9718	6.4710	11.3810
C_2	7.0495	15.2341	26.7317

virtual elements with an over-penalization strategy as an extension of [8] for the discontinuous Galerkin schemes. A disadvantage is the quantification of the restriction on the stabilization parameter in practise and poor condition for larger parameters. The stabilization-free a posteriori error control in this paper is based on two observations for the HHO schemes on simplicial triangulations. First, the P_1-conforming finite element functions let the stabilization vanish and, second, the divergence-free lowest-order Raviart-Thomas functions are L^2 perpendicular to the piecewise gradients $\nabla_{\mathrm{pw}} Ru_h$. In fact, those two fairly general properties lead in Sect. 2 to a reliable explicit residual-based a posteriori error estimator. In contrast to the simplified introduction above, the paper also focuses on multiplicative constants that lead to the GUB

$$\text{error} \leq \eta_{\mathrm{res}} \quad \text{and error} \leq \eta_{\mathrm{eq},p};$$

cf. Table 1 for explicit quantities and Theorem 1 and Theorem 3 for further details.

Numerical comparisons of η_{HHO} with η_{res} and $\eta_{\mathrm{eq},p}$ favour the latter. Section 2 identifies general building blocks of the a posteriori error analysis for discontinuous schemes with emphasis on explicit constants. An application to HHO leads to the new stabilization-free residual-based estimator η_{res} in Sect. 3. The alternative stabilization-free error estimator $\eta_{\mathrm{eq},p}$ follows from an equilibration strategy plus post-processing in Sect. 4. This paper also contributes to the HHO literature a local equivalence of two stabilizations and the efficiency of the stabilization terms up to data-oscillations in extension of [32]. Numerical comparisons of the different error estimators and an error estimator competition for guaranteed error control of the piecewise energy norm in 2D conclude this paper in Sect. 5. Three computational benchmarks provide striking numerical evidences for the optimality of the associated adaptive algorithms. The appendix provides algorithmic details on the computation of the post-processed contribution $\|Q_p - \nabla_{\mathrm{pw}} Ru_h\|_{L^2(\Omega)}$ in $\eta_{\mathrm{eq},p}$.

1.4 Overall notation

Standard notation for Sobolev and Lebesgue spaces and norms apply with $\|\bullet\| := \|\bullet\|_{L^2(\Omega)}$ and $|||\bullet||| := \|\nabla \bullet\|_{L^2(\Omega)}$. In particular, $H(\mathrm{div}, \Omega)$ is the space of Sobolev functions with weak divergence in $L^2(\Omega)$ and $H(\mathrm{div} = 0, \Omega)$ contains only divergence-free functions in $H(\mathrm{div}, \Omega)$. Throughout this paper, $\mathcal{T}$ denotes a shape-regular triangulation of the polyhedral bounded Lipschitz domain $\Omega \subset \mathbb{R}^n$ into n-simplices with facets $\mathcal{F}$ (edges for $n = 2$ and faces for $n = 3$) and ver-

tices $\mathcal{V}$. Let $\mathcal{F}(\Omega)$ (resp. $\mathcal{V}(\Omega)$) denote the set of interior facets (resp. vertices) and $\mathcal{F}(\partial\Omega) := \mathcal{F}\backslash\mathcal{F}(\partial\Omega)$ (resp. $V(\partial\Omega) := \mathcal{V}\backslash\mathcal{V}(\Omega)$). Given $v \in \Omega \to \mathbb{R}^n$ and $w : \Omega \to \mathbb{R}^{2n-3}$, let $\operatorname{curl} v := \partial_1 v_2 - \partial_2 v_1$ and $\operatorname{Curl} w := (\partial_2 w, -\partial_1 w)^t$ if $n = 2$ and $\operatorname{curl} v := (\partial_2 v_3 - \partial_3 v_2, \partial_3 v_1 - \partial_1 v_3, \partial_1 v_2 - \partial_2 v_1)^t$ and $\operatorname{Curl} w := \operatorname{curl} w$ if $n = 3$. For $s \in \mathbb{R}$, let $H^s(\mathcal{T})$, $H(\operatorname{div}, \mathcal{T})$, and $H(\operatorname{curl}, \mathcal{T})$ denote the space of piecewise Sobolev functions with restriction to $T \in \mathcal{T}$ in $H^s(T)$, $H(\operatorname{div}, T)$, and $H(\operatorname{curl}, T)$. To simplify notation, $H^s(K)$ abbreviates $H^s(\operatorname{int}(K))$ for the open interior $\operatorname{int}(K)$ of a compact set K. The L^2-scalar product reads $(\bullet, \bullet)_{L^2(\omega)}$ for volumes $\omega \subseteq \Omega$ and $\langle \bullet, \bullet \rangle_{L^2(\gamma)}$ for surfaces $\gamma \subset \overline{\Omega}$ of co-dimension one; the same symbol applies to scalars and to vectors. For $V := H^1_0(\Omega)$ and $V^* := H^{-1}(\Omega)$, let $\langle \bullet, \bullet \rangle$ denote the duality-brackets in $V^* \times V$ for the dual space V^* of V equipped with the operator norm $|||F|||_* := \sup_{v \in V\backslash\{0\}} |Fv|/|||v|||$ for $F \in V^*$.

Define the energy scalar product $a(v, w) := (\nabla v, \nabla w)_{L^2(\Omega)}$ for $v, w \in H^1(\Omega)$ and its piecewise version $a_{\mathrm{pw}}(v, w) = (\nabla_{\mathrm{pw}} v, \nabla_{\mathrm{pw}} w)_{L^2(\Omega)}$ for $v, w \in H^1(\mathcal{T})$. The latter induces the seminorm $|||\bullet|||_{\mathrm{pw}} := a_{\mathrm{pw}}(\bullet, \bullet)^{1/2}$ in $H^1(\mathcal{T})$. Here and throughout the paper, ∇_{pw}, $\operatorname{div}_{\mathrm{pw}}$, $\operatorname{curl}_{\mathrm{pw}}$, Δ_{pw}, denote the piecewise evaluation of the differential operators ∇, div, $\operatorname{curl}_{\mathrm{pw}}$, Δ without explicit reference to the underlying shape-regular triangulation $\mathcal{T}$.

The vector space $P_k(K)$ of polynomials of degrees at most $k \in \mathbb{N}_0$ over a facet or simplex $K \in \mathcal{F} \cup \mathcal{T}$ defines the piecewise polynomial spaces

$$P_k(\mathcal{T}) := \{p \in L^2(\Omega) \ : \ p_{|T} \in P_k(T) \text{ for all } T \in \mathcal{T}\},$$
$$P_k(\mathcal{F}) := \{p \in L^2(\mathcal{F}) \ : \ p_{|F} \in P_k(F) \text{ for all } F \in \mathcal{F}\}$$

and the space of piecewise Raviart-Thomas functions

$$RT_k^{\mathrm{pw}}(\mathcal{T}) := P_k(\mathcal{T}; \mathbb{R}^n) + x P_k(\mathcal{T}).$$

The associated L^2 projections read $\Pi_{K,k} : L^2(\Omega) \to P_k(K)$, $\Pi_k : L^2(\Omega) \to P_k(\mathcal{T})$, and $\Pi_{\mathcal{F},k} : L^2(\Omega) \to P_k(\mathcal{F})$ with the convention $\Pi_{-1} := 0$. Abbreviate $S_0^{k+1}(\mathcal{T}) := P_{k+1}(\mathcal{T}) \cap V$ and $RT_k(\mathcal{T}) := RT_k^{\mathrm{pw}}(\mathcal{T}) \cap H(\operatorname{div}, \Omega)$ for all $k \in \mathbb{N}_0$. The piecewise constant mesh-size function $h_{\mathcal{T}} \in P_0(\mathcal{T})$ satisfies $h_{\mathcal{T}|T} := h_T$ for $T \in \mathcal{T}$ with the diameter $h_K := \operatorname{diam}(K) \in P_0(K)$ of $K \in \mathcal{F} \cup \mathcal{T}$.

If not explicitly stated otherwise, constants are independent of the mesh-size in the triangulation but may depend on the shape-regularity and on the polynomial degree k. The abbreviation $A \lesssim B$ hides a generic constant C (independent of the mesh-size) in $A \le C\ B$; $A \approx B$ abbreviates $A \lesssim B \lesssim A$.

2 Foundations of the a posteriori error analysis

This section investigates general building blocks of the a posteriori error analysis and revisits arguments from [14, 18, 20, 21] with emphasis on multiply connected domains $\Omega \subset \mathbb{R}^n$ for $n = 2, 3$. The general setting of this section results in reliability for an error estimator that is applicable beyond the HHO methodology. Consider the weak

solution $u \in V = H_0^1(\Omega)$ to the Poisson model problem $-\Delta u = f$ a.e. in Ω and $u = 0$ on $\partial\Omega$ for a given source $f \in L^2(\Omega)$; i.e., $u \in V$ satisfies

$$a(u, v) = (f, v)_{L^2(\Omega)} \quad \text{for all } v \in V. \tag{3}$$

An approximation $G \in L^2(\Omega; \mathbb{R}^n)$ of the gradient $\nabla u \in H(\mathrm{div}, \Omega)$ gives rise to the residual $f + \mathrm{div}\, G \in V^* = H^{-1}(\Omega)$ seen as a linear functional on V, i.e.,

$$\langle f + \mathrm{div}\, G, \varphi\rangle := (f, \varphi)_{L^2(\Omega)} - (G, \nabla\varphi)_{L^2(\Omega)} \quad \text{for all } \varphi \in V.$$

Let ν_T denote the unit outer normal along the boundary ∂T of each simplex $T \in \mathcal{T}$ and fix the orientation of a unit normal $\nu_F = \pm\nu_T$ for each facet $F \in \mathcal{F}(T)$ of T such that it matches the outer unit normal ν of $\partial\Omega$ at the boundary. The jump $[G]_F$ of a piecewise function in $m \in \mathbb{N}$ components $G \in H^1(\mathcal{T}; \mathbb{R}^m)$ reads $[G]_F := G_{|T_+} - G_{|T_-}$ on interior facets $F = T_+ \cap T_- \in \mathcal{F}(\Omega)$ (with $T_\pm$ labelled such that $\nu_{T_+|F} = \nu_F = -\nu_{T_-|F}$) and $[G]_F := G$ on the boundary $F \in \mathcal{F}(\partial\Omega)$. The main result of this section establishes the residual-based error estimator

$$\begin{aligned}\eta^2(\mathcal{T}, G) := &\left(C_1\|h_{\mathcal{T}}(f + \mathrm{div}_{\mathrm{pw}} G)\| + C_2\sqrt{\sum_{F\in\mathcal{F}(\Omega)} \ell(F)\|[G]_F \cdot \nu_F\|^2_{L^2(F)}}\right)^2 \\ &+ C_{\mathrm{H}}^2\left(C_1\|h_{\mathcal{T}}\mathrm{curl}_{\mathrm{pw}} G\| + C_2\sqrt{\sum_{F\in\mathcal{F}} \ell(F)\|[G]_F \times \nu_F\|^2_{L^2(F)}}\right)^2\end{aligned} \tag{4}$$

as a GUB $\|\nabla u - G\| \le \eta(\mathcal{T}, G)$ under minimal assumptions on the approximation $G \in H^1(\mathcal{T}; \mathbb{R}^n) \subset L^2(\Omega; \mathbb{R}^n)$. The constants C_1, C_2, and C_H (or upper bounds thereof) are computable; cf. Table 1 for an example in 2D with details in Example 1 at the end of Sect. 2. The first assumption is a weakened discrete solution property

$$(G, \nabla w_C)_{L^2(\Omega)} = (f, w_C)_{L^2(\Omega)} \quad \text{for all } w_C \in S_0^1(\mathcal{T}). \tag{5}$$

The second assumption is the orthogonality to the lowest-order divergence-free Raviart-Thomas functions

$$(G, r)_{L^2(\Omega)} = 0 \quad \text{for all } r \in RT_0(\mathcal{T}) \cap H(\mathrm{div} = 0, \Omega). \tag{6}$$

Theorem 1 (residual-based GUB) *Suppose that $G \in H^1(\mathcal{T}; \mathbb{R}^n)$ and $f \in L^2(\Omega)$ satisfy (5)–(6). Then the error estimator $\eta(\mathcal{T}, G)$ from (4) is a GUB*

$$\|\nabla u - G\| \le \eta(\mathcal{T}, G)$$

of the error $\|\nabla u - G\|$ for the solution $u \in V$ to (3). The constants C_1, C_2, C_{H} exclusively depend on Ω and the shape-regularity of $\mathcal{T}$.

The remaining parts of this section are devoted to the proof of Theorem 1 and the computation of (upper bounds of) the constants C_1, C_2, and C_{H} in (4). The point of departure is the subsequent decomposition that appears necessary in the nonconforming and mixed finite element a posteriori error analysis. It leads to a split of the error $\|\nabla u - G\|$ into some divergence part and some consistency part.

Lemma 1 (decomposition) *Any $v \in V$ and $G \in L^2(\Omega;\mathbb{R}^n)$ satisfy the decomposition*

$$\|\nabla v - G\|^2 = |||v - w|||^2 + \|G - \nabla w\|^2 \tag{7}$$

with the (unique) minimizer $w \in V$ of the distance

$$\delta := \min_{\varphi \in V} \|G - \nabla \varphi\|$$

of G to the gradients ∇V of Sobolev functions. The solution $u \in V$ to (3) satisfies

$$\begin{aligned} \mu := |||f + \operatorname{div} G|||_* = |||u - w||| \quad \text{and} \\ \|\nabla u - G\|^2 = |||f + \operatorname{div} G|||_*^2 + \|G - \nabla w\|^2 = \mu^2 + \delta^2. \end{aligned} \tag{8}$$

Proof The minimizer $w \in V$ of $\|G - \nabla\varphi\|$ among $\varphi \in V$ satisfies the variational formulation $a(w,\varphi)_{L^2(\Omega)} = (G, \nabla\varphi)_{L^2(\Omega)}$ for all $\varphi \in V$. (Notice that w is the unique weak solution to the Poisson model problem $-\Delta w = -\operatorname{div} G \in V^*$.) In particular, $G - \nabla w$ is L^2 orthogonal onto ∇V and the Pythagoras theorem proves (7). Given $\varphi \in V$ with $|||\varphi||| = 1$, the orthogonality of $G - \nabla w$ to $\nabla\varphi$ and (3) show

$$a(u - w, \varphi)_{L^2(\Omega)} = (\nabla u - G, \nabla\varphi)_{L^2(\Omega)} = \langle f + \operatorname{div} G, \varphi\rangle \tag{9}$$

with the duality brackets $\langle \bullet, \bullet\rangle$ in $V^* \times V$. Since the supremum of (9) over all $\varphi \in V$ with $|||\varphi||| = 1$ is equal to $|||u - w||| = |||f + \operatorname{div} G|||_*$, this and (7) conclude the proof of (8). □

The split (7) of the error $\|\nabla u - G\|$ allows for and enforces a separate estimation of the equilibrium and consistency contribution in residual-based a posteriori error estimators.

In order to derive explicit constants, two lemmas are recalled. The first has a long tradition in the a posteriori error control in form of a Helmholtz decomposition on simply connected domains [4, 13] and introduces the constant C_{H} from Theorem 1. The following version includes the general case of multiply connected domains as in [33] for $n = 2$ or $n = 3$ dimensions and weak assumptions on a divergence-free function $\varrho \in H(\operatorname{div} = 0, \Omega)$.

Lemma 2 (Helmholtz-decomposition) *Suppose the divergence-free function $\varrho \in H(\operatorname{div} = 0, \Omega)$ is L^2 orthogonal onto $RT_0(\mathcal{T}) \cap H(\operatorname{div} = 0, \Omega)$. Then there exists $\beta \in H^1(\Omega;\mathbb{R}^N)$, $N = 2n - 3$, such that any $\beta_C \in S^1(\mathcal{T})^N$ satisfies*

$$\|\varrho\|^2 = \int_\Omega \varrho \cdot \operatorname{Curl}(\beta - \beta_C)\, \mathrm{d}x \quad \text{and} \quad |||\beta||| \le C_{\mathrm{H}} \|\varrho\|. \tag{10}$$

The constant $C_{\mathrm{H}} > 0$ exclusively depends on Ω.

Proof The compact polyhedral boundary $\partial\Omega$ of the bounded Lipschitz domain Ω has $J+1$ connectivity components $\Gamma_0, \ldots, \Gamma_J$ for some finite $J \in \mathbb{N}_0$. Those connectivity components have a positive surface measure $|\Gamma_j|$ and a positive distance of each other. So the integral mean

$$\gamma_j := \int_{\Gamma_j} \varrho \cdot \nu \, \mathrm{d}s/|\Gamma_j|$$

is well defined and depends continuously on $\varrho \in H(\mathrm{div} = 0, \Omega)$ in the sense that $|\gamma_j| \leq c_1 \|\varrho\|$ (recall $\mathrm{div}\, \varrho = 0$) for each $j = 0, \ldots, J$ and $c_1 > 0$. This constant c_1 and the constants c_2, c_3, c_4 below exclusively depend on the domain Ω. The finite real numbers $\gamma_0, \ldots, \gamma_J$ define the Neumann data for the harmonic function $z \in H^1(\Omega)/\mathbb{R}$ with

$$\Delta z = 0 \text{ in } \Omega \quad \text{and} \quad \partial z/\partial \nu = \gamma_j \text{ on } \Gamma_j \text{ for all } j = 0, \ldots, J.$$

The elliptic regularity theory for polyhedral domains lead to $z \in H^{1+\alpha}(\Omega)$ for some $\alpha > 1/2$ and $c_2 > 0$ with $\|z\|_{H^{1+\alpha}(\Omega)} \leq c_2 (|\gamma_0| + \cdots + |\gamma_J|)$. The Raviart-Thomas interpolation operator defines a bounded linear operator on $H(\mathrm{div}, \Omega) \cap L^p(\Omega; \mathbb{R}^n)$ for $p > 2$. It is generally accepted that, for $\alpha > 0$ and $\nabla z \in H(\mathrm{div} = 0, \Omega) \cap H^\alpha(\Omega; \mathbb{R}^n)$, the Fortin interpolation $I_{\mathrm{F}} \nabla z \in RT_0(\mathcal{T}) \cap H(\mathrm{div} = 0, \Omega)$ is well defined and $\|I_{\mathrm{F}} \nabla z\| \leq c_3 \|\nabla z\|_{H^\alpha(\Omega)}$ follows for some $c_3 > 0$. The additional property $\nabla z \in L^p(\Omega; \mathbb{R}^n)$ for some $p > 2$ allows the definition of $\int_F \nabla z \cdot \nu_F \, \mathrm{d}s$ as a Lebesgue integral over a facet $F \in \mathcal{F}$. One consequence for the boundary facets is the vanishing integral

$$\int_{\Gamma_j} (\varrho - I_{\mathrm{F}} \nabla z) \cdot \nu \, \mathrm{d}s = 0 \quad \text{for all } j = 0, \ldots, J.$$

Since $\varrho - I_{\mathrm{F}} \nabla z \in H(\mathrm{div} = 0, \Omega)$ is divergence-free, Theorems 3.1 and 3.4 in [33] prove the existence of $c_4 > 0$ and $\beta \in H^1(\Omega; \mathbb{R}^N)$ with

$$\varrho = I_{\mathrm{F}} \nabla z + \mathrm{Curl}\, \beta \quad \text{and} \quad |||\beta||| \leq c_4 \|\varrho - I_{\mathrm{F}} \nabla z\|.$$

Recall that $\varrho \perp I_{\mathrm{F}} \nabla z$ and $\varrho \perp \mathrm{curl}\, \beta_C \in RT_0(\mathcal{T}) \cap H(\mathrm{div} = 0, \Omega)$. This concludes the proof of (10) with $C_{\mathrm{H}} := \sqrt{1 + (c_1 c_2 c_3 (1+J))^2} c_4$. □

The subsequent version of the trace inequality on the facets $\mathcal{F}$ leads to the piecewise constant $\ell \in P_0(\mathcal{F})$ defined by

$$\ell(F) := \begin{cases} (n+1) h_T^2 |F|/|T| & \text{for } F \in \mathcal{F}(\partial\Omega) \cap \mathcal{F}(T), \\ (n+1)|F|/(h_{T_+}^{-2}|T_+| + h_{T_-}^{-2}|T_-|) & \text{for } F = \partial T_+ \cap \partial T_- \in \mathcal{F}(\Omega). \end{cases}$$

Lemma 3 (trace inequality) *Any* $f \in H^1(\Omega)$ *satisfies*

$$\sum_{F\in\mathcal{F}} \ell(F)^{-1} \|f\|^2_{L^2(F)} \leq \left\|h_{\mathcal{T}}^{-1} f\right\|^2 + \frac{2C_{\mathrm{tr}}}{n} \left\|h_{\mathcal{T}}^{-1} f\right\| |||f|||$$

with the constant $C_{\mathrm{tr}} := \max_{T\in\mathcal{T}} \max_{x\in T} |x - \mathrm{mid}(T)|/h_T < n/(n+1)$.

Proof The center of inertia $\mathrm{mid}(T) = \sum_{j=0}^n P_j/(n+1)$ of the n-simplex $T = \mathrm{conv}\{P_0, ..., P_n\} \in \mathcal{T}$ and the $n+1$ faces $F_j = \mathrm{conv}\{P_0, ..., P_{j-1}, P_{j+1}, ..., P_n\} \in \mathcal{F}(T)$ for $j = 0, ..., n$ give rise to the decomposition of T into $n+1$ sub-simplices $T'_j = \mathrm{conv}(F_j, \mathrm{mid}(T))$ with volume

$|T'_j| = |T|/(n+1)$.

Standard arguments like the trace identity on $T'_j \subset T$ [17, Lemma 2.1] for $|f|^2 \in W^{1,1}(T')$ and a Cauchy inequality show

$$\frac{1}{|F_j|} \|f\|^2_{L^2(F_j)} \leq \frac{1}{|T'_j|} \|f\|^2_{L^2(T'_j)} + \frac{2}{n|T'_j|} \max_{x\in T'_j} |x - \mathrm{mid}(T)| \, \|f\|_{L^2(T'_j)} \|\nabla f\|_{L^2(T')}.$$

The distance $\max_{x\in T'_j} |x - \mathrm{mid}(T)| = |P_k - \mathrm{mid}(T)| \leq C_{\mathrm{tr}} h_T$ is attained at a vertex P_k for $k \in \{0, ..., j-1, j+1, ..., n\}$. Since the centroid $\mathrm{mid}(T)$ divides each median of T in the ratio n to 1 and the length of each median is strictly bounded by h_T,

the bound $C_{\mathrm{tr}} < n/(n+1)$ follows and cannot be improved in the absence of further assumptions on the shape of the simplex T. Since $|T'_j| = |T|/(n+1)$, the previously displayed estimate leads to

$$\frac{|T|}{(n+1)h_T^2|F_j|} \|f\|^2_{L^2(F_j)} \leq \left\|h_T^{-1} f\right\|^2_{L^2(T'_j)} + \frac{2C_{\mathrm{tr}}}{n} \left\|h_T^{-1} f\right\|_{L^2(T'_j)} \|\nabla f\|_{L^2(T'_j)}.$$

Let $\mathcal{T}'$ be the refinement of $\mathcal{T}$, obtained by replacing $T \in \mathcal{T}$ with $T'_0, ..., T'_d$ from above. The triangulation $\mathcal{T}'$ allows for the facet based decomposition $\{\omega'(F)\}_{F\in\mathcal{F}}$ of Ω, where $\omega'(F)$ is either the patch $\omega'(F) = \mathrm{int}(T'_+ \cup T'_-)$ for an interior facet $F = T'_+ \cap T'_-$ or $\omega'(F) = \mathrm{int}(T')$ for $F \in \mathcal{F}(\partial\Omega) \cap \mathcal{F}(T')$. This establishes, for any $F \in \mathcal{F}$, the estimate

$$\ell(F)^{-1} \|f\|^2_{L^2(F)} \leq \left\|h_{\mathcal{T}}^{-1} f\right\|^2_{L^2(\omega'(F))} + \frac{2C_{\mathrm{tr}}}{n} \left\|h_{\mathcal{T}}^{-1} f\right\|_{L^2(\omega'(F))} \|\nabla f\|_{L^2(\omega'(F))}.$$

Since the family $\{\omega'(F) : F \in \mathcal{F}\}$ has no overlap, the sum of the last displayed inequality over all $F \in \mathcal{F}$ and a Cauchy inequality conclude the proof of Lemma 3. □

The next lemma utilizes a quasi-interpolation operator $J : H^1(\Omega) \to S^1(\mathcal{T})$ with the restriction $J(V) \subset S^1_0(\mathcal{T})$, e.g., $J = J_1 \circ I_{NC}$ from [19, Section 5] with explicit constants for $n = 2$, and the approximation and stability properties

$$\left\|h_{\mathcal{T}}^{-1}(\varphi - J\varphi)\right\| \leq C_1 |||\varphi||| \quad \text{and} \quad |||\varphi - J\varphi||| \leq C_{\mathrm{st}} |||\varphi||| \tag{11}$$

for constants C_1 and C_{st} exclusively depending on the shape-regularity of $\mathcal{T}$. For the precise definition of J_1 and I_{NC}, we refer to [19, eq. (47) and Section 5]. Recall the constant C_{tr} from Lemma 3 and set $C_2 := (C_1(C_1 + 2C_{\mathrm{tr}}C_{\mathrm{st}}/n))^{1/2}$.

Lemma 4 (equilibrium) *Suppose that $G \in H(\mathrm{div}, \mathcal{T})$ and $f \in L^2(\Omega)$ satisfy (5) and suppose $(G|_T)|_F \cdot \nu_F \in L^2(F)$ for all $F \in \mathcal{F}(T)$ and $T \in \mathcal{T}$. Then*

$$|||f + \mathrm{div}\, G|||_* \leq C_1 \|h_{\mathcal{T}}(f + \mathrm{div}_{\mathrm{pw}} G)\| + C_2 \sqrt{\sum_{F \in \mathcal{F}(\Omega)} \ell(F) \|[G]_F \cdot \nu_F\|^2_{L^2(F)}}.$$

Proof Given $\varphi \in V$ with $|||\varphi||| = 1$, set $\psi := \varphi - \varphi_C$ for some quasi-interpolation $\varphi_C := J\varphi \in S^1_0(\mathcal{T})$ with (11). Since (5) implies $\langle f + \mathrm{div}\, G, \varphi\rangle = \langle f + \mathrm{div}\, G, \psi\rangle$, a piecewise integration by parts and the collection of jump contributions show

$$\langle f + \mathrm{div}\, G, \varphi\rangle = (f + \mathrm{div}_{\mathrm{pw}} G, \psi)_{L^2(\Omega)} - \sum_{F \in \mathcal{F}(\Omega)} \langle [G]_F \cdot \nu_F, \psi\rangle_{L^2(F)}. \tag{12}$$

The first bound follows from a Cauchy inequality and (11),

$$\begin{aligned}(f + \mathrm{div}_{\mathrm{pw}} G, \psi)_{L^2(\Omega)} &\leq \|h_{\mathcal{T}}(f + \mathrm{div}_{\mathrm{pw}} G)\|\, \|h_{\mathcal{T}}^{-1}\psi\| \\ &\leq C_1 \|h_{\mathcal{T}}(f + \mathrm{div}_{\mathrm{pw}} G)\|\, |||\varphi|||. \end{aligned} \tag{13}$$

The second bound additionally exploits the trace inequality of Lemma 3,

$$\begin{aligned}&\sum_{F \in \mathcal{F}(\Omega)} \langle [G]_F \cdot \nu_F, \psi\rangle_{L^2(F)} \\ &\quad\leq \sqrt{\sum_{F \in \mathcal{F}(\Omega)} \ell(F) \|[G]_F \cdot \nu_F\|^2_{L^2(F)}} \sqrt{\sum_{F \in \mathcal{F}(\Omega)} \ell(F)^{-1} \|\psi\|^2_{L^2(F)}} \\ &\quad\leq \sqrt{{C_1}^2 + \frac{2C_{\mathrm{tr}}}{n} C_{\mathrm{st}} C_1} \sqrt{\sum_{F \in \mathcal{F}(\Omega)} \ell(F) \|[G]_F \cdot \nu_F\|^2_{L^2(F)}} \end{aligned} \tag{14}$$

with $|||\varphi||| = 1$ in the last step. Since (13)–(14) hold for all $\varphi \in V$ with $|||\varphi||| = 1$, the supremum in (12) over all such φ concludes the proof. □

The final ingredient for the proof of Theorem 1 controls the second term δ in the decomposition of Lemma 1 for $\varrho := G - \nabla w$. Recall C_{H} from Lemma 2 and C_1 from (11), and C_2 from page 9.

Lemma 5 (conformity) *Suppose the divergence-free function $\varrho \in H(\mathrm{div} = 0, \Omega) \cap H(\mathrm{curl}, \mathcal{T})$ is L^2 orthogonal onto $RT_0(\mathcal{T}) \cap H(\mathrm{div} = 0, \Omega)$ and satisfies $(\varrho|_T)|_F \times \nu_F \in L^2(F)$ for all $F \in \mathcal{F}(T)$ and $T \in T$. Then*

$$C_{\mathrm{H}}^{-1} \|\varrho\| \leq C_1 \|h_{\mathcal{T}} \mathrm{curl}_{\mathrm{pw}} \varrho\| + C_2 \sqrt{\sum_{F \in \mathcal{F}} \ell(F) \|[\varrho]_F \times \nu_F\|^2_{L^2(F)}}.$$

Proof Lemma 2 provides $\beta \in H^1(\Omega;\mathbb{R}^N)$ with (10) for a (component-wise) quasi-interpolation $\beta_C \in S^1(\mathcal{T})^N$ with (11) as in the proof of Lemma 4; set $\psi := \beta - \beta_C$. A piecewise integration by parts and the collection of jump contributions shows

$$\|\varrho\|^2 = \int_\Omega \varrho \cdot \operatorname{Curl}(\beta - \beta_C)dx = \int_\Omega \psi \cdot \operatorname{curl}_{\mathrm{pw}}\varrho \, dx + \sum_{F\in\mathcal{F}} \int_F \psi[\varrho]_F \times \nu_F \, ds.$$

Stability and approximation properties of the quasi-interpolation (11) and the trace inequality of Lemma 3 eventually lead to

$$\|\varrho\|^2 \le C_1 \left\| h_{\mathcal{T}} \operatorname{curl}_{\mathrm{pw}}\varrho \right\| |||\beta||| + C_2 \sqrt{\sum_{F\in\mathcal{F}} \ell(F) \|[\varrho]_F \times \nu_F\|^2_{L^2(F)}}\, |||\beta|||.$$

In fact, the routine estimation with element and jump terms is completely analogous to the proof of Lemma 4 and leads to the same constants C_1, C_2. This and $|||\beta||| \le C_{\mathrm{H}}\|\varrho\|$ conclude the proof. □

Proof (Theorem 1) The trace of $G|_T \in H^1(T;\mathbb{R}^n)$ is well defined on any facet $F \in \mathcal{F}(T)$ of the simplex $T \in \mathcal{T}$. Lemma 1 provides $w \in V = H^1_0(\Omega)$ with $\|\nabla u - G\|^2 = |||f + \operatorname{div} G|||^2_* + \|G - \nabla w\|^2$. Since G satisfies (5), Lemma 4 establishes

$$|||f + \operatorname{div} G|||_* \le C_1 \|h_{\mathcal{T}}(f + \operatorname{div}_{\mathrm{pw}} G)\| + C_2 \sqrt{\sum_{F\in\mathcal{F}(\Omega)} \ell(F) \|[G]_F \cdot \nu_F\|^2_{L^2(F)}}.$$

The assumption (6) on G and an integration by parts prove that Lemma 5 is applicable to $\varrho := G - \nabla w \in H(\operatorname{div} = 0, \Omega) \cap H(\operatorname{curl}, \mathcal{T}; \mathbb{R}^n)$. Since $\operatorname{curl} \nabla w = 0$ and $\nabla w \times \nu = 0$, this reveals

$$C_{\mathrm{H}}^{-1} \|G - \nabla w\| \le C_1 \|h_{\mathcal{T}} \operatorname{curl}_{\mathrm{pw}} G\| + C_2 \sqrt{\sum_{F\in\mathcal{F}} \ell(F) \|[G]_F \times \nu_F\|^2_{L^2(F)}}.$$

The above estimates together with the decomposition of Lemma 1 establish $\eta(\mathcal{T}, G)$ as a GUB for the error $\|\nabla u - G\|$. □

Example 1 (constants for right-isosceles triangles) In two space dimensions, $\|\operatorname{Curl} \bullet\| = |||\bullet|||$ and so $C_{\mathrm{H}} \le 1$ for a simply connected domain Ω in Lemma 2. The choice $J := J_1 \circ I_{\mathrm{NC}}$ from [19, Section 5] of the quasi-interpolation operator J in the proof of Lemma 4 allows for the explicit estimates

$$C_1 \le \sqrt{48^{-1} + j_{1,1}^{-2} + c_{\mathrm{apx}}^2} \text{ and } C_{\mathrm{st}} \le 1 + \sqrt{72} c_{\mathrm{apx}},$$

where $j_{1,1} = 3.8317$ denotes the first positive root of the first Bessel function. For triangulations into right-isosceles triangles, the constant $c_{\mathrm{apx}} \le \sqrt{3}/(2 - 2\cos(\pi/\max\{4, M_{\mathrm{bd}}\}))$ from [19, Lemma 4.8] depends on the domain by the maximal number $M_{\mathrm{bd}} \le 4\max\{\pi, \omega_{\max}\}/\pi \le 8$ of triangles sharing a boundary vertex.

Given the maximal interior angle $\omega_{\max}$ of Ω, Table 1 displays those constants for the maximal possible value $M_{\mathrm{bd}} = 4\max\{\pi, \omega_{\max}\}/\pi$. The geometric quantity $\max_{x\in T} |x - \mathrm{mid}(T)|$ equals two-thirds of the maximum median of T. Thus, $C_{\mathrm{tr}} = \sqrt{5}/(3\sqrt{2}) \leq 0.5271$ and $\ell(F) = 6h_F$ for interior edges $F \in \mathcal{F}(\Omega)$ and $\ell(F) = 12h_F$ for boundary edges $F \in \mathcal{F}(\partial\Omega)$ of triangulations into right-isosceles triangles. Consequently,

$$C_1 \leq \sqrt{48^{-1} + j_{1,1}^{-2} + c_{\mathrm{apx}}^2} =: C_{\mathcal{T}}, \tag{15}$$

$$C_2 \leq \sqrt{C_{\mathcal{T}}(C_{\mathcal{T}} + 0.5271(1 + \sqrt{72}c_{\mathrm{apx}}))} =: C_{\mathcal{F}}. \tag{16}$$

3 Explicit residual-based a posteriori HHO error estimator

The arguments from Sect. 2 apply to the HHO method and result in a stabilization-free reliable a posteriori error control. In combination with the efficiency estimate from this section, this leads to a new explicit residual-based a posteriori error estimator for the HHO method that is equivalent to the error up to data oscillations.

3.1 Hybrid high-order methodology

The HHO ansatz space reads $V_h := P_k(\mathcal{T}) \times P_k(\mathcal{F}(\Omega))$ for $k \in \mathbb{N}_0$ with the subspace $P_k(\mathcal{F}(\Omega)) \subset P_k(\mathcal{F})$ of piecewise polynomials $p \in P_k(\mathcal{F})$ under the convention $p_{|\partial\Omega} = 0$. The interpolation $\mathrm{I} : V \to V_h$ maps $v \in V$ onto $\mathrm{I}v := (\Pi_k v, \Pi_{\mathcal{F},k} v) \in V_h$. Given any $v_h = (v_{\mathcal{T}}, v_{\mathcal{F}}) \in V_h$, the reconstruction operator $R : V_h \to P_{k+1}(\mathcal{T})$ defines the unique piecewise polynomial $Rv_h \in P_{k+1}(\mathcal{T})$ with $\Pi_0(Rv_h - v_{\mathcal{T}}) = 0$ such that, for all $w_{k+1} \in P_{k+1}(\mathcal{T})$,

$$\begin{aligned} &a_{\mathrm{pw}}(Rv_h, w_{k+1}) \\ &\quad = a_{\mathrm{pw}}(v_{\mathcal{T}}, w_{k+1}) - \sum_{T\in\mathcal{T}} \langle v_{\mathcal{T}|T} - v_{\mathcal{F}}, \nabla w_{k+1|T} \cdot \nu_T \rangle_{L^2(\partial T)}. \end{aligned} \tag{17}$$

Let $u_h \in V_h$ solve the HHO discrete formulation of (3) with

$$a_h(u_h, v_h) = (f, v_{\mathcal{T}})_{L^2(\Omega)} \qquad \text{for all } v_h = (v_{\mathcal{T}}, v_{\mathcal{F}}) \in V_h \tag{18}$$

for the HHO bilinear form

$$a_h(u_h, v_h) := a_{\mathrm{pw}}(Ru_h, Rv_h) + s_h(u_h, v_h) \tag{19}$$

and the stabilization term $s_h(u_h, v_h)$ from (2). Given any $w_C \in S_0^1(\mathcal{T}) = P_1(\mathcal{T}) \cap H_0^1(\Omega)$, the definition of the reconstruction operator R in (17) verifies $R\mathrm{I}w_C = w_C$ with the interpolation I onto V_h. Hence, $S_{TF}\mathrm{I}w_C = 0$ vanishes for all $F \in \mathcal{F}(T)$ and

$T \in \mathcal{T}$. This and (18) show, for all $w_C \in S^1_0(\mathcal{T})$, that

$$a_{\mathrm{pw}}(Ru_h, w_C) = (f, \Pi_k w_C)_{L^2(\Omega)} = (\Pi_k f, w_C)_{L^2(\Omega)}. \tag{20}$$

3.2 Explicit a posteriori error estimator

As a result of (20), $\nabla_{\mathrm{pw}} Ru_h$ satisfies the solution property (5) if $k \geq 1$ and, in the lowest order case $k = 0$, (5) holds with f replaced by $\Pi_0 f$. This allows the application of the theory from Sect. 2 to the HHO method with minor modifications for the case $k = 0$. Define the error estimator contributions

$$\begin{aligned}
\eta^2_{\mathrm{res},1}(\mathcal{T}) &:= \begin{cases} \|h_{\mathcal{T}}(f + \Delta_{\mathrm{pw}} Ru_h)\|^2 & \text{for } k \geq 1, \\ \|h_{\mathcal{T}} \Pi_0 f\|^2 & \text{for } k = 0, \end{cases} \\
\eta^2_{\mathrm{res},2}(\mathcal{T}) &:= \begin{cases} 0 & \text{for } k \geq 1, \\ \mathrm{osc}^2_0(f, \mathcal{T}) & \text{for } k = 0, \end{cases} \\
\eta^2_{\mathrm{res},3}(\mathcal{T}) &:= \sum_{F \in \mathcal{F}(\Omega)} \ell(F) \|[\nabla_{\mathrm{pw}} Ru_h]_F \cdot \nu_F\|^2_{L^2(F)}, \\
\eta^2_{\mathrm{res},4}(\mathcal{T}) &:= \sum_{F \in \mathcal{F}} \ell(F) \|[\nabla_{\mathrm{pw}} Ru_h]_F \times \nu_F\|^2_{L^2(F)}.
\end{aligned} \tag{21}$$

Since $\nabla_{\mathrm{pw}} Ru_h$ is a piecewise gradient, its piecewise curl vanishes. This leads to the explicit residual-based a posteriori error estimator

$$\eta^2_{\mathrm{res}}(\mathcal{T}) := \big(C_1 \eta_{\mathrm{res},1}(\mathcal{T}) + C_P \eta_{\mathrm{res},2}(\mathcal{T}) + C_2 \eta_{\mathrm{res},3}(\mathcal{T})\big)^2 + C^2_{\mathrm{H}} C^2_2 \eta^2_{\mathrm{res},4}(\mathcal{T}). \tag{22}$$

(Recall C_1, C_2 from Lemma 4 and C_{H} from Lemma 2 as well as the Poincaré constant $C_P \leq \pi^{-1}$.) The main result of this section verifies the assumptions in Theorem 1 and proves reliability and efficiency of $\eta_{\mathrm{res}}(\mathcal{T})$.

Theorem 2 (residual-based GUB for HHO) *Let $u \in V$ solve the Poisson equation (3) and let $u_h \in V_h$ solve the discrete formulation (18). Then*

$$|||u - Ru_h|||_{\mathrm{pw}} \leq \eta_{\mathrm{res}}(\mathcal{T}) \leq C_3\big(|||u - Ru_h|||_{\mathrm{pw}} + \mathrm{osc}_q(f, \mathcal{T})\big)$$

and $\mathrm{osc}_{k-1}(f, \mathcal{T}) \leq C_4 \eta_{\mathrm{res}}(\mathcal{T})$ hold for any $q \in \mathbb{N}_0$. The constants C_3 and C_4 exclusively depend on k, q and on the shape-regularity of the triangulation $\mathcal{T}$.

3.3 Proof of Theorem 2

The orthogonality of $\nabla_{\mathrm{pw}} Ru_h$ to the divergence-free Raviart-Thomas space of lowest degree is an assumption in Theorem 1 and verified below.

Lemma 6 (orthogonality) *The piecewise gradients $\nabla_{\mathrm{pw}} RV_h$ are L^2 orthogonal to the space $RT_0(\mathcal{T}) \cap H(\mathrm{div} = 0, \Omega)$, i.e., any $v_h \in V_h$ and $q_{RT} \in RT_0(\mathcal{T}) \cap H(\mathrm{div} =$*

0, Ω) *satisfy*

$$(\nabla_{\mathrm{pw}} R v_h, q_{RT})_{L^2(\Omega)} = 0. \tag{23}$$

Proof Given any $q_{RT} \in RT_0(\mathcal{T}) \cap H(\mathrm{div} = 0, \Omega)$, $\mathrm{div}\, q_{RT} = 0$ shows $q_{RT} \in P_0(\mathcal{T}; \mathbb{R}^n)$ [28, Lemma 14.9]. Since $P_0(\mathcal{T}; \mathbb{R}^n) = \nabla_{\mathrm{pw}} P_1(\mathcal{T})$, there exists a piecewise affine function $\phi_1 \in P_1(\mathcal{T})$ with $q_{RT} = \nabla_{\mathrm{pw}} \phi_1$ a.e. in Ω. This and the definition of $R v_h$ from (17) imply, for any $v_h = (v_{\mathcal{T}}, v_{\mathcal{F}}) \in V_h$, that

$$\begin{aligned}(\nabla_{\mathrm{pw}} R v_h, q_{RT})_{L^2(\Omega)} &= a_{\mathrm{pw}}(R v_h, \phi_1) \\ &= a_{\mathrm{pw}}(v_{\mathcal{T}}, \phi_1) - \sum_{T \in \mathcal{T}} \langle v_{\mathcal{T}}|_T - v_{\mathcal{F}}, \nabla_{\mathrm{pw}} \phi_1 \cdot \nu_T \rangle_{L^2(\partial T)}.\end{aligned}$$

This, a piecewise integration by parts, and $\Delta_{\mathrm{pw}} \phi_1 \equiv 0$ lead to

$$\begin{aligned}(\nabla_{\mathrm{pw}} R v_h, q_{RT})_{L^2(\Omega)} &= \sum_{T \in \mathcal{T}} \langle v_{\mathcal{F}}, \nabla_{\mathrm{pw}} \phi_1 \cdot \nu_T \rangle_{L^2(\partial T)} \\ &= \sum_{F \in \mathcal{F}} \langle v_{\mathcal{F}}, [q_{RT} \cdot \nu_F]_F \rangle_{L^2(F)}. \end{aligned} \tag{24}$$

Since $q_{RT} \in RT_0(\mathcal{T})$ has continuous normal components, the jump term $\langle v_{\mathcal{F}}, [q_{RT}]_F \cdot \nu_F \rangle_{L^2(F)} = 0$ vanishes for all $F \in \mathcal{F}(\Omega)$. This, $v_{\mathcal{F}} \equiv 0$ on $\partial\Omega$, and (24) conclude $(\nabla_{\mathrm{pw}} R v_h, q_{RT})_{L^2(\Omega)} = 0$. □

The following lemma concerns the efficiency of the jump contributions. Each facet $F \in \mathcal{F}$ has at most two adjacent simplices that define a triangulation $\mathcal{T}(F) := \{T \in \mathcal{T} : F \in \mathcal{F}(T)\}$ of the facet-patch $\omega(F) := \mathrm{int}(\bigcup_{T \in \mathcal{T}(F)} T)$.

Lemma 7 (efficiency of jumps) *The solution $u \in V$ to (3) and the discrete solution $u_h \in V_h$ to (18) satisfy (a) for all $F \in \mathcal{F}$ and (b) for all $F \in \mathcal{F}(\Omega)$.*

(a) $h_F^{1/2} \|[\nabla_{\mathrm{pw}} R u_h]_F \times \nu_F\|_{L^2(F)} \lesssim \min_{v \in V} \|\nabla v - \nabla_{\mathrm{pw}} R u_h\|_{L^2(\omega(F))}$,

(b) $h_F^{1/2} \|[\nabla_{\mathrm{pw}} R u_h]_F \cdot \nu_F\|_{L^2(F)} \lesssim \|\nabla u - \nabla_{\mathrm{pw}} R u_h\|_{L^2(\omega(F))} + \mathrm{osc}_k(f, \mathcal{T}(F))$.

Proof The proof is based on the following extension argument. Given a polynomial $p \in P_k(F)$ of degree at most k along the side $F \in \mathcal{F}$, the coefficients determine a polynomial (also denoted by p) along the hyperplane H that enlarges F. The intersection $\widehat{F} := H \cap \mathrm{conv}(\omega(F))$ of the hyperplane H with the convex hull of the facet-patch $\omega(F)$ may be strictly larger than F. The shape-regularity of $\mathcal{T}$ bounds the size of $\widehat{F}$ in terms of F and an inverse estimate leads to a bound $\|p\|_{L^\infty(\widehat{F})} \le C(k) \|p\|_{L^\infty(F)}$ with a constant $C(k)$ that depends on the shape-regularity of $\mathcal{T}$ and on k. The extension of p from H to $\mathbb{R}^n$ by constant values along the side normal ν_F leads to a polynomial $\widehat{p} \in P_k(\mathbb{R}^n)$ with

$$\|\widehat{p}\|_{L^\infty(\omega(F))} \le \|p\|_{L^\infty(\widehat{F})} \le C(k) \|p\|_{L^\infty(F)}. \tag{25}$$

Proof of (a). The tangential jump $\varrho_F := [\nabla_{\mathrm{pw}} R v_h]_F \times \nu_F \in P_k(F;\mathbb{R}^N)$ is a polynomial in $N = 2n-3$ components on $F \in \mathcal{F}$ for $n = 2, 3$. Let $p = \varrho_F(j)$ be one of the components of $\varrho_F \in P_k(F)^N$, for $j = 1, ..., N$, and extend it as explained above to $\hat{p} \in P_k(\mathbb{R}^n)$ and call this $\widehat{\varrho}(j)$ in the vector $\widehat{\varrho_F} \in P_k(\mathbb{R}^n;\mathbb{R}^N)$. The proof involves the piecewise polynomial facet-bubble function $b_F := n^n \Pi_{j=1}^n \varphi_j$ for the n nodal basis function $\varphi_1, \ldots, \varphi_n \in S^1(\mathcal{T})$ associated with the vertices of F. An inverse estimate [38, Proposition 3.37] shows

$$\|\varrho_F\|_{L^2(F)}^2 \lesssim \|b_F^{1/2}\varrho_F\|_{L^2(F)}^2 = \langle b_F\varrho_F, \varrho_F\rangle_{L^2(F)}. \tag{26}$$

Since $\varrho := b_F\widehat{\varrho_F} \in S_0^{k+n}(\mathcal{T}(F);\mathbb{R}^N)$ vanishes on $\partial\omega(F)\backslash\mathrm{int}(F)$, (26) and a piecewise integration by parts show

$$\|\varrho_F\|_{L^2(F)}^2 \lesssim \langle \varrho, [\nabla_{\mathrm{pw}} R v_h]_F \times \nu_F\rangle_{L^2(F)} = (\mathrm{curl}\,\varrho, \nabla_{\mathrm{pw}} R v_h)_{L^2(\omega(F))}. \tag{27}$$

This and $(\mathrm{curl}\,\varrho, \nabla v)_{L^2(\Omega)} = 0$ for any $v \in V$ imply

$$\begin{aligned}\|\varrho_F\|_{L^2(F)}^2 &\lesssim (\mathrm{curl}\,\varrho, \nabla_{\mathrm{pw}}(R v_h - v))_{L^2(\omega(F))}\\ &\le \|\mathrm{curl}\,\varrho\|_{L^2(\omega(F))}\|\nabla_{\mathrm{pw}}(R v_h - v)\|_{L^2(\omega(F))}.\end{aligned} \tag{28}$$

An inverse estimate, $\|b_F\|_{L^\infty(\omega(F))} = 1$, and (25) imply

$$\begin{aligned}\|\mathrm{curl}\,\varrho\|_{L^2(\omega(F))} &\lesssim \|\nabla\varrho\|_{L^2(\omega(F))} \lesssim h_F^{-1+n/2}\|\varrho\|_{L^\infty(\omega(F))}\\ &\lesssim h_F^{-1+n/2}h_F^{-(n-1)/2}\|\varrho_F\|_{L^2(F)} = h_F^{-1/2}\|\varrho_F\|_{L^2(F)}.\end{aligned} \tag{29}$$

In combination with (28), this concludes the proof of (a).

Proof of (b). The efficiency of normal jumps (b) follows from the arguments for conforming FEMs, cf. [38, Section 1.4.5]; further details are omitted. □

The following lemma reveals that the order $k \ge \mathbb{N}_0$ of the oscillations $\mathrm{osc}_k(f,T)$ in Lemma 7 (b) can be any natural number. It is certainly known to the experts but hard to find in the literature. Recall the convention $\Pi_{-1} := 0$.

Lemma 8 (efficiency of lower-order oscillations) *Given any simplex $T \in \mathcal{T}$ and parameters $k, q \in \mathbb{N}_0$, the solution $u \in V$ to (3) satisfies*

$$C_5^{-1}\mathrm{osc}_{k-1}^2(f,T) \le \min_{v_{k+1}\in P_{k+1}(T)} \|\nabla_{\mathrm{pw}}(u - v_{k+1})\|_{L^2(T)}^2 + \mathrm{osc}_q^2(f,T). \tag{30}$$

The constant C_5 exclusively depends on q and the shape of T.

Proof The assertion (30) is trivial for $q \le k-1$, so suppose $k \le q$. Any $v_{k+1} \in P_{k+1}(T)$ and $\varrho_T := \Pi_q f + \Delta v_{k+1} \in P_q(T)$ satisfy

$$\mathrm{osc}_{k-1}^2(f,T) \le h_T^2\|f + \Delta v_{k+1}\|_{L^2(T)}^2 = \mathrm{osc}_q^2(f,T) + h_T^2\|\varrho_T\|_{L^2(T)}^2. \tag{31}$$

Let $b_T \in S_0^{n+1}(T)$ with $0 \leq b_T \leq 1 = \max b_T$ denote the volume bubble-function on $T \in \mathcal{T}$. The equivalence of norms in the finite-dimensional space $P_q(T)$ provides

$$\|b_T^{1/2} \varrho_T\|_{L^2(T)} \leq \|\varrho_T\|_{L^2(T)} \leq C_6 \|b_T^{1/2} \varrho_T\|_{L^2(T)}. \tag{32}$$

A more detailed analysis of the mass matrices reveals that the constant C_6 exclusively depends on the polynomial degree q. An integration by parts with $b_T \varrho_T \in S_0^{q+n+1}(T) \subset V$ and the weak formulation (3) result in

$$\begin{aligned} \|b_T^{1/2} \varrho_T\|_{L^2(T)}^2 &= (\Pi_q f + \Delta v_{k+1}, b_T \varrho_T)_{L^2(T)} \\ &= (\nabla(u - v_{k+1}), \nabla(b_T \varrho_T))_{L^2(T)} - (f - \Pi_q f, b_T \varrho_T)_{L^2(T)}. \end{aligned}$$

A Cauchy inequality, the inverse estimate $h_T \|\nabla(b_T \varrho_T)\|_{L^2(T)} \leq C_7 \|\varrho_T\|_{L^2(T)}$ with a constant C_7 that exclusively depends on $q + n + 1$ and the shape of T, and (32) lead to

$$C_6^{-2} h_T \|\varrho_T\|_{L^2(T)} \leq C_7 \|\nabla(u - v_{k+1})\|_{L^2(T)} + \operatorname{osc}_q(f, T) \tag{33}$$

The combination of (31) with (33) and a Cauchy inequality conclude the proof of (30), e.g., with $C_5 = 1 + {C_6}^4 (1 + {C_7}^2)$. □

Proof (of Theorem 2) Recall the definition of $\eta_{\mathrm{res}}(\mathcal{T})$ for $k \geq 1$ and $k = 0$ in (21). Since $\operatorname{osc}_{k-1}^2(f, \mathcal{T}) \leq \eta_{\mathrm{res},1}^2(\mathcal{T}) + \eta_{\mathrm{res},2}^2(\mathcal{T}) \lesssim \eta_{\mathrm{res}}^2(\mathcal{T})$, the remaining parts of this proof discuss the reliability and efficiency of $\eta_{\mathrm{res}}(\mathcal{T})$.

Lemma 6 provides the orthogonality of $\nabla_{\mathrm{pw}} R u_h \in H^1(\mathcal{T}; \mathbb{R}^n)$ to the divergence-free Raviart-Thomas function $RT_0(\mathcal{T}) \cap H(\mathrm{div} = 0, \Omega)$. This and (20) show that the assumptions in Theorem 1 hold for $G := \nabla_{\mathrm{pw}} R u_h$ and $k \geq 1$, whence the reliability of $\eta_{\mathrm{res}}(\mathcal{T})$ follows with a reliability constant 1.

Minor modifications to the proof of Theorem 1 lead to reliability in the case $k = 0$. In fact, the only modifications required concern the upper bound of $|||f + \mathrm{div}\, \nabla_{\mathrm{pw}} R u_h|||_* \leq |||(1 - \Pi_0) f|||_* + |||\Pi_0 f + \mathrm{div}\, \nabla_{\mathrm{pw}} R u_h|||_*$. A piecewise Poincaré inequality shows $|||(1 - \Pi_0) f|||_* \leq C_P \operatorname{osc}_0(\mathcal{T}, f)$ with the Poincaré constant $C_P (\leq 1/\pi$ for simplices). Lemma 4 proves $|||\Pi_0 f + \mathrm{div}\, \nabla_{\mathrm{pw}} R u_h|||_* \leq C_1 \eta_{\mathrm{res},1}(\mathcal{T}) + C_2 \eta_{\mathrm{res},3}(\mathcal{T})$. Hence, the decomposition of Lemma 1 and Lemma 5 result in $|||u - R u_h|||_{\mathrm{pw}} \leq \eta_{\mathrm{res}}(\mathcal{T})$.

This provides the reliability and it remains to verify the efficiency $\eta_{\mathrm{res}}(\mathcal{T}) \lesssim |||u - R u_h|||_{\mathrm{pw}} + \operatorname{osc}_q(f, \mathcal{T})$ for any $q \in \mathbb{N}_0$. The Pythagoras theorem and (33) with $\varrho_T := \Pi_k f + \Delta R u_h \in P_k(T)$ and $v_{k+1} := R u_h \in P_{k+1}(T)$ lead to the local efficiency of the volume contributions

$$\begin{aligned} \|h_T (f + \Delta_{\mathrm{pw}} R u_h)\|_{L^2(T)}^2 &= \operatorname{osc}_k^2(f, T) + \|h_T \varrho_T\|_{L^2(T)}^2 \\ &\lesssim \|\nabla(u - R u_h)\|_{L^2(T)}^2 + \operatorname{osc}_k^2(f, T). \end{aligned}$$

Lemma 7 considers the remaining terms in the error estimator and establishes their efficiency namely,

$$\sum_{F\in\mathcal{F}} h_F\|[\nabla_{\mathrm{pw}}Ru_h]_F\|_{L^2(F)} \lesssim |||u - Ru_h|||_{\mathrm{pw}} + \mathrm{osc}_k(f,\mathcal{T})$$

with the modified jump $[\nabla_{\mathrm{pw}}Ru_h]_F = \nabla_{\mathrm{pw}}Ru_h \times \nu_F$ on boundary facets $F \in \mathcal{F}(\partial\Omega)$. This and Lemma 8 establish the existence of some mesh-independent constant $C_3 > 0$ with $C_3^{-1}\eta_{\mathrm{res}}(\mathcal{T}) \le |||u - Ru_h|||_{\mathrm{pw}} + \mathrm{osc}_q(f,\mathcal{T})$ for arbitrary $q \in \mathbb{N}_0$. This concludes the proof. □

While the focus of this paper is on the HHO methodology, the framework of Sect. 2 also applies to other skeletal methods as well. The following example covers a hybridized discontinuous Galerkin (HDG) FEM from [35] with the Lehrenfeld-Schöberl stabilization.

Example 2 (HDG FEM) Let $V_h := P_{k+1}(\mathcal{T}) \times P_k(\mathcal{F}(\Omega))$ for $k \in \mathbb{N}_0$. An equivalent formulation to the HDG FEM from [35] seeks $u_h \in V_h$ with

$$a_{\mathrm{pw}}(Ru_h, Rv_h) + s_h(u_h, v_h) = (f, v_{\mathcal{T}}) \quad \text{for any} v_h = (v_{\mathcal{T}}, v_{\mathcal{F}}) \in V_h.$$

Here, $R : V_h \to P_{k+1}(\mathcal{T})$ is defined as in (17) and

$$s_h(v_h, w_h) := \sum_{T\in\mathcal{T}} \sum_{F\in\mathcal{F}(T)} h_F^{-1}\langle \Pi_{F,k}(v_{\mathcal{T}}|_T - v_{\mathcal{F}}|_F), w_{\mathcal{T}}|_T - w_{\mathcal{F}}|_F\rangle_{L^2(F)}$$

for any $v_h = (v_{\mathcal{T}}, v_{\mathcal{F}})$, $w_h = (w_{\mathcal{T}}, w_{\mathcal{F}}) \in V_h$. This method is also known under the label of weak Galerkin FEM [39]. It is straightforward to verify that $\nabla_{\mathrm{pw}}Ru_h$ satisfies (5)–(6). Notice that (5) also holds for $k = 0$ without any modification. Therefore, Theorem 1 leads to the reliable a posteriori estimate

$$|||u - Ru_h|||_{\mathrm{pw}}^2 \le \eta_{\mathrm{res}}^2(\mathcal{T}) := \|h_{\mathcal{T}}(f + \Delta_{\mathrm{pw}}Ru_h)\|^2 + \sum_{F\in\mathcal{F}(\Omega)} \ell(F)\|[\nabla_{\mathrm{pw}}Ru_h]_F \cdot \nu_F\|_{L^2(F)}^2 + \sum_{F\in\mathcal{F}} \ell(F)\|[\nabla_{\mathrm{pw}}Ru_h]_F \times \nu_F\|_{L^2(F)}^2.$$

The efficiency $\eta_{\mathrm{res}}(\mathcal{T}) \lesssim |||u - Ru_h|||_{\mathrm{pw}}$ follows from the arguments in the proofs of Lemma 7–8.

4 Equilibrium-based a posteriori HHO error analysis

The residual-based guaranteed upper bound (GUB) of the error $|||u - Ru_h|||_{\mathrm{pw}}$ from Sect. 3.2 employs explicit constants that may lead to overestimation in higher dimensions and for different triangular shapes. This section utilizes equilibrated flux reconstructions [1, 2, 5, 6, 30] to establish, up to the well-known Poincaré constant $C_P \le 1/\pi$, a constant-free guaranteed upper bounds for a tight error control.

4.1 Guaranteed error control

The guaranteed upper bounds of this section involves two post-processings of the potential reconstruction $Ru_h \in P_{k+1}(\mathcal{T})$ of the discrete solution u_h to (18). First, the patch-wise design of a flux reconstruction $Q_p \in RT_{k+p}(\mathcal{T})$ with $p \in \mathbb{N}_0$ from [3, 10, 31] provides an $H(\mathrm{div}, \Omega)$-conforming approximation to $\nabla_{\mathrm{pw}} Ru_h$ with the equilibrium $\Pi_r f + \mathrm{div}\, Q_p = 0$ in Ω and r from (35) below. Second, the nodal average $\mathcal{A}Ru_h \in S_0^{k+1}(\mathcal{T}) \subset V$ results in an V-conforming approximation of Ru_h by averaging all values of the discontinuous function Ru_h at each Lagrange point of $S_0^{k+1}(\mathcal{T})$. This, the split (7), and the solution property (20) give rise to the guaranteed upper bound (GUB)

$$\eta_{\mathrm{eq},p}^2(\mathcal{T}) := \big(C_P \mathrm{osc}_r(f, \mathcal{T}) + \|Q_p - \nabla_{\mathrm{pw}} Ru_h\|\big)^2 + |||(1 - \mathcal{A})Ru_h|||_{\mathrm{pw}}^2 \tag{34}$$

with $r \in \mathbb{N}_0$ defined by

$$r := 0 \text{ if } k = 0 \quad \text{and} \quad r := k + p \text{ if } k \geq 1. \tag{35}$$

The main result of this section states the reliability and efficiency (up to data oscillations) of $\eta_{\mathrm{eq},p}$ for all parameters $p \in \mathbb{N}_0$.

Theorem 3 (equilibrium-based GUB for HHO) *Let $u \in V$ resp. $u_h \in V_h$ solve (3) resp. (18). Given a parameter $p \in \mathbb{N}_0$, there exists $Q_p \in RT_{k+p}(\mathcal{T})$ such that the error estimator $\eta_{\mathrm{eq},p}(\mathcal{T})$ from (34) is an efficient GUB*

$$|||u - Ru_h|||_{\mathrm{pw}} \leq \eta_{\mathrm{eq},p}(\mathcal{T}) \leq C_8\big(|||u - Ru_h|||_{\mathrm{pw}} + \mathrm{osc}_q(f, \mathcal{T})\big). \tag{36}$$

for any $q \in \mathbb{N}_0$ and $\mathrm{osc}_{k-1}(f, \mathcal{T}) \leq C_9 \eta_{\mathrm{eq},p}(\mathcal{T})$.

The constants C_8 and C_9 exclusively depend on the polynomial degree $k \in \mathbb{N}_0$, the parameter $q \in \mathbb{N}_0$, and the shape-regularity of $\mathcal{T}$.

At least two technical contributions for the proof of Theorem 3 are of broader interest. A first contribution to the HHO literature is the local equivalence of the original HHO stabilization s_h from (2) and the alternative stabilization $\tilde{s}_h(v_h, v_h) := \sum_{T \in \mathcal{T}} \tilde{s}_T(v_h, v_h)$ from [25] defined, for $v_h = (v_{\mathcal{T}}, v_{\mathcal{F}}) \in V_h$, by

$$\begin{aligned} \tilde{s}_T(v_h, v_h) := {} & h_T^{-2} \|\Pi_{T,k}(v_{\mathcal{T}} - Rv_h)\|_{L^2(T)}^2 \\ & + \sum_{F \in \mathcal{F}(T)} h_F^{-1} \|\Pi_{F,k}(v_{\mathcal{F}} - Rv_h|_T)\|_{L^2(F)}^2. \end{aligned} \tag{37}$$

A second result of separate interest in the HHO literature (cf. [25] where the efficiency in (38) is left open) is the efficiency of the stabilizations from Theorems 4–5 below,

$$\tilde{s}_h(v_h, v_h)^{1/2} \approx s_h(u_h, u_h)^{1/2} \lesssim |||u - Ru_h|||_{\mathrm{pw}} + \mathrm{osc}_{k+p}(f, \mathcal{T}). \tag{38}$$

The subsequent subsection continues with some explanations on the flux reconstruction $Q_p \in RT_{k+p}(\mathcal{T})$ that is defined by local minimization problems on each vertex patch. Appendix A complements the discussion with an algorithmic two-step procedure for the computation of $Q_p - \nabla_{\mathrm{pw}} Ru_h$ in 2D. The efficiency of the averaging $|||(1-\mathcal{A})Ru_h|||_{\mathrm{pw}}$ up to data oscillations follows in Sects. 4.3–4.4. Section 4.6 concludes with the proof of Theorem 3.

4.2 Construction of equilibrated flux

This subsection defines the post-processed $H(\mathrm{div},\Omega)$-conforming equilibrated flux $Q_p \in RT_{k+p}(\mathcal{T})$ that enters the GUB $\eta_{\mathrm{eq},p}$ from (34) based on local patch-wise minimization problems in the spirit of [10, 30, 31].

Consider the shape-regular vertex-patch $\omega(z) := \mathrm{int}(\bigcup\{T \in \mathcal{T}(z)\})$ covered by the neighbouring simplices $\mathcal{T}(z) := \{T \in \mathcal{T} : z \in T\}$ sharing a given vertex $z \in \mathcal{V}$ with the facet spider $\mathcal{F}(z) := \{F \in \mathcal{F}\ z \in F\}$. Recall the space of piecewise Raviart-Thomas functions $RT_k^{\mathrm{pw}}(\mathcal{T})$ from Sect. 1.4 and define

$$
\begin{aligned}
L_0^2(\omega(z)) &:= \{f \in L^2(\omega(z)) : (f,1)_{L^2(\omega(z))} = 0\},\\
L_*^2(\omega(z)) &:= \begin{cases} L_0^2(\omega(z)) & \text{if } z \in \mathcal{V}(\Omega),\\ L^2(\omega(z)) & \text{else,}\end{cases}\\
H_*^1(\omega(z)) &:= \begin{cases} H^1(\omega(z)) \cap L_0^2(\omega(z)) & \text{if } z \in \mathcal{V}(\Omega),\\ \{v \in H^1(\omega(z)) : v = 0 \text{ on } \partial\Omega \cap \bigcup \mathcal{F}(z)\} & \text{else,}\end{cases}\\
H_0(\mathrm{div},\omega(z)) &:= \begin{cases} \{r \in H(\mathrm{div},\omega(z)) : r\cdot\nu = 0 \text{ on } \partial\omega(z)\} & \text{if } z \in \mathcal{V}(\Omega),\\ \{r \in H(\mathrm{div},\omega(z)) : r\cdot\nu = 0 \text{ on } \partial\omega(z)\setminus\bigcup\mathcal{F}(z)\} & \text{else,}\end{cases}\\
RT_k^0(\mathcal{T}(z)) &:= RT_k^{\mathrm{pw}}(\mathcal{T}(z)) \cap H_0(\mathrm{div},\omega(z)).
\end{aligned}
$$

Throughout the remaining parts of this section, abbreviate $G_h := \nabla_{\mathrm{pw}} Ru_h \in P_k(\mathcal{T};\mathbb{R}^n)$. Given a vertex $z \in \mathcal{V}$ with the P_1-conforming nodal basis function $\varphi_z \in S^1(\mathcal{T})$, the property (20) provides compatible data

$$
f_z := \begin{cases} \Pi_p(\varphi_z \Pi_0 f - G_h\cdot\nabla\varphi_z) & \text{if } k=0,\\ \Pi_{k+p}(\varphi_z f - G_h\cdot\nabla\varphi_z) & \text{if } k\geq 1\end{cases} \in L_*^2(\omega(z)) \tag{39}
$$

such that the discrete affine space

$$
\mathcal{Q}_h(z) := \{\tau_z \in RT_{k+p}^0(\mathcal{T}(z)) \ :\ \mathrm{div}\,\tau_z + f_z = 0 \text{ in } \Omega\} \neq \emptyset \tag{40}
$$

is not empty. Consequently,

$$
Q_{z,h} := \operatorname*{arg\,min}_{\tau_z\in\mathcal{Q}_h(z)} \|\tau_z - \mathcal{I}_{RT}(\varphi_z G_h)\|_{L^2(\omega(z))} = \Pi_{\mathcal{Q}_h(z)}\mathcal{I}_{RT}(\varphi_z G_h) \tag{41}
$$

is well defined as the L^2 projection $\Pi_{\mathcal{Q}_h(z)}\mathcal{I}_{RT}(\varphi_z G_h)$ of $\mathcal{I}_{RT}(\varphi_z G_h)$ onto $\mathcal{Q}_h(z)$ with the piecewise Raviart-Thomas interpolation $\mathcal{I}_{RT} : H^1(\mathcal{T};\mathbb{R}^n) \to RT^{\mathrm{pw}}_{k+p}(\mathcal{T})$ [7, Section III.3.1]. In the case $p \geq 1$, $\varphi_z G_h \in P_{k+1}(\mathcal{T}(z)) \subset RT^{\mathrm{pw}}_{k+p}(\mathcal{T}(z))$ is a piecewise Raviart-Thomas function of degree $k+p$. Hence $\mathcal{I}_{RT}(\varphi_z G_h) = \varphi_z G_h$ and $\mathcal{I}_{RT}$ could be omitted in the formula (41). The partition of unity $\sum_{z\in\mathcal{V}} \varphi_z \equiv 1$ and $G_h = \mathcal{I}_{RT} G_h = \sum_{z\in\mathcal{V}} \mathcal{I}_{RT}(\varphi_z G_h)$ show that the sum $Q_p = \sum_{z\in\mathcal{V}} Q_{z,h} \in H(\mathrm{div},\Omega)$ of the patch-wise contributions satisfies

$$\mathrm{div}\, Q_p = \begin{cases} \sum_{z\in\mathcal{V}} \Pi_p(G_h\cdot\nabla\varphi_z - \varphi_z \Pi_0 f) = -\Pi_0 f & \text{if } k=0, \\ \sum_{z\in\mathcal{V}} \Pi_{k+p}(G_h\cdot\nabla\varphi_z - \varphi_z f) = -\Pi_{k+p} f & \text{if } k\geq 1, \end{cases} \tag{42}$$

$$\|Q_p - G_h\|^2_{L^2(\Omega)} \lesssim \sum_{z\in\mathcal{V}} \|Q_{z,h} - \mathcal{I}_{RT}(\varphi_z G_h)\|^2_{L^2(\omega(z))}. \tag{43}$$

This establishes the flux reconstruction Q_p. The efficiency of the flux reconstruction will be based on the following general equivalence.

Lemma 9 (control of $H(\mathrm{div})$ minimization by residual [10, 31]) *Given any vertex $z \in \mathcal{V}$, a piecewise Raviart-Thomas function $\sigma_z \in RT^{\mathrm{pw}}_q(\mathcal{T}(z))$ and a piecewise polynomial $r_z \in P_q(\mathcal{T}(z))$ of degree $q \in \mathbb{N}_0$, define the residual*

$$\mathrm{Res}_z(v) := \sum_{T\in\mathcal{T}(z)} \Big((r_z, v)_{L^2(T)} + \langle \sigma_z\cdot\nu_T, v\rangle_{L^2(\partial T)} \Big) \tag{44}$$

for all $v \in H^1(\Omega)$. If $z \in \mathcal{V}(\Omega)$ is an interior vertex, then suppose additionally that $\mathrm{Res}_z(1) = 0$. Then

$$\min_{\substack{\tau_z\in RT^0_q(\mathcal{T}(z)) \\ \mathrm{div}\tau_z = r_z + \mathrm{div}_{\mathrm{pw}}\sigma_z}} \|\tau_z - \sigma_z\|_{L^2(\omega(z))} \leq C_{\mathrm{s}} \max_{\substack{v\in H^1_*(\omega(z)) \\ \|\nabla v\|_{L^2(\omega(z))}=1}} \mathrm{Res}_z(v) \tag{45}$$

holds for a constant C_{s} that exclusively depends on the shape-regularity (and is in particular independent of the polynomial degree q).

Proof The assertion follows from [10, Theorem 7] in $n = 2$ dimensions and [31, Corollaries 3.3, 3.6, and 3.8] in $n = 3$ dimensions. □

Remark 1 The patch-wise construction of Q_p in Sect. 4.2 typically generates local data oscillation $\mathrm{osc}_{k+p}(\varphi_z f, \mathcal{T}(z))$ in the error analysis as in the proof of Theorem 3 in Sect. 4.6 below or, e.g., [30, Theorem 3.17]. A straightforward computation $\mathrm{osc}_{k+p}(\varphi_z f, \mathcal{T}(z)) \leq \mathrm{osc}_{k+p-1}(f, \mathcal{T}(z))$ apparently leads to a loss of one degree in the data oscillation but Lemma 8 verifies

$$\mathrm{osc}^2_{k+p}(\varphi_z f, \mathcal{T}(z)) \lesssim \min_{v_h\in P_{k+1}(\mathcal{T}(z))} \|\nabla_{\mathrm{pw}}(u - v_h)\|^2_{L^2(\omega(z)} + \mathrm{osc}^2_q(f, \mathcal{T}(z)) \tag{46}$$

for any $p, q \in \mathbb{N}_0$. This allows for efficiency of the data oscillations on the right-hand side of the efficiency estimate [30, Formula (3.42)] and leads to a corresponding refinement in [30, Theorem 3.17].

4.3 Local equivalence of stabilizations

The first improvement to the current HHO literature is the local equivalence of the two stabilizations $\tilde{s}_h$ from (37) and s_h from (2). The authors of this paper could not find any motivation for the alternative stabilization $\tilde{s}_h$ in the error analysis of [25, Section 4] and suggest to apply Theorem 4 below to [25, Theorem 4.7] to recover the results therein for the original HHO stabilization s_h. Recall the local stabilization $\tilde{s}_T$ in $\tilde{s}_h(v_h, v_h) := \sum_{T\in\mathcal{T}} \tilde{s}_T(v_h, v_h)$ from (37) and $S_{TF} v_h = \Pi_{F,k}\left(v_\mathcal{T} + (1 - \Pi_{T,k}) R v_h\right)|_T - v_\mathcal{F}|_F$ in the definition of s_h from (2).

Theorem 4 (local equivalence of stabilizations) *Any $v_h = (v_\mathcal{T}, v_\mathcal{F}) \in V_h$ and $T \in \mathcal{T}$ satisfy*

$$C_{10}{}^{-1} \tilde{s}_T(v_h, v_h) \leq \sum_{F\in\mathcal{F}(T)} h_F^{-1} \|S_{TF} v_h\|^2_{L^2(F)} \leq C_{11} \tilde{s}_T(v_h, v_h). \tag{47}$$

The constants C_10 and C_11 exclusively depend on the polynomial degree k and the shape regularity of $\mathcal{T}$.

Proof The second inequality in (47) follows directly from a triangle inequality and an inverse estimate. Therefore, the proof focuses on the first inequality in (47). Given $v_h = (v_\mathcal{T}, v_\mathcal{F}) \in V_h$ and $T \in \mathcal{T}$, let $\varphi_k := (\Pi_k R v_h - v_\mathcal{T})|_T \in P_k(T)$. Since $S_{TF} v_h = \Pi_{F,k}(R v_{h|T} - v_\mathcal{F}|_F - \varphi_k)$, the triangle inequality $\|\Pi_{F,k}(R v_{h|T} - v_\mathcal{F})\|_{L^2(F)} \leq \|S_{TF} v_h\|_{L^2(F)} + \|\varphi_k\|_{L^2(F)}$, the discrete trace inequality $\|\varphi_k\|_{L^2(F)} \lesssim h_F^{-1/2} \|\varphi_k\|_{L^2(T)}$, and the shape-regularity $h_F \approx h_T$ for all $F \in \mathcal{F}(T)$ reveal

$$\begin{aligned} &\sum_{F\in\mathcal{F}(T)} h_F^{-1} \|\Pi_{F,k}(R v_{h|T} - v_\mathcal{F})\|^2_{L^2(F)} \\ &\quad\lesssim \sum_{F\in\mathcal{F}(T)} h_F^{-1} \|S_{TF} v_h\|^2_{L^2(F)} + h_T^{-2} \|\varphi_k\|^2_{L^2(T)}. \end{aligned} \tag{48}$$

Since $\Pi_0 \varphi_k = 0$ (from the design of $R v_h$), a Poincaré inequality shows

$$h_T^{-2} \|\varphi_k\|^2_{L^2(T)} \leq C_P^2 \|\nabla \varphi_k\|^2_{L^2(T)}. \tag{49}$$

On the one hand, an integration by parts provides

$$\|\nabla \varphi_k\|^2_{L^2(T)} = -(\Pi_k R v_h - v_\mathcal{T}, \Delta \varphi_k)_{L^2(T)} + \langle \varphi_k, \nabla \varphi_k \cdot \nu_T \rangle_{L^2(\partial T)}. \tag{50}$$

On the other hand, an integration by parts and the definition of R imply

$$-(R v_h, \Delta \varphi_k)_{L^2(T)} = (\nabla R v_h, \nabla \varphi_k)_{L^2(T)} - \langle R v_{h|T}, \nabla \varphi_k \cdot \nu_T \rangle_{L^2(\partial T)}$$

$$= -(v_{\mathcal{T}}, \Delta\varphi_k)_{L^2(T)} + \sum_{F\in\mathcal{F}(T)} \langle v_{\mathcal{F}} - Rv_{h|T}, \nabla\varphi_k \cdot \nu_T\rangle_{L^2(F)}. \tag{51}$$

Since $\Delta\varphi_k \in P_k(T)$, the L^2 projection Π_k on the right-hand side of (50) is redundant. Hence, the combination of (50)–(51) with $\nabla\varphi_k \cdot \nu_{T|F} \in P_k(F)$ for all $F \in \mathcal{F}(T)$ results in

$$\|\nabla\varphi_k\|^2_{L^2(T)} = \sum_{F\in\mathcal{F}(T)} \langle \Pi_{F,k}(v_{\mathcal{F}} - Rv_{h|T} + \varphi_k), \nabla\varphi_k \cdot \nu_T\rangle_{L^2(F)}. \tag{52}$$

A Cauchy inequality on the right-hand side of (52), a discrete trace inequality, and $S_{TF}v_h = \Pi_{F,k}(Rv_{h|T} - v_{\mathcal{F}|F} - \varphi_k)$ for all $F \in \mathcal{F}(T)$ lead to

$$\|\nabla\varphi_k\|^2_{L^2(T)} \lesssim \sum_{F\in\mathcal{F}(T)} h_F^{-1}\|S_{TF}v_h\|^2_{L^2(F)}. \tag{53}$$

Since $\tilde{s}_T(v_h, v_h) = \sum_{F\in\mathcal{F}(T)} h_F^{-1}\|\Pi_{F,k}(Rv_{h|T} - v_{\mathcal{F}})\|^2_{L^2(F)} + h_T^{-2}\|\varphi_k\|^2_{L^2(T)}$, the combination of (48)–(49) with (53) concludes the proof of (47). □

4.4 Efficiency of the stabilization

The second improvement to the HHO literature is a quasi-best approximation estimate along the lines of the seminal paper [32, Theorem 4.10]. In combination with Theorem 4, this, in particular, provides the efficiency (38) of the stabilization up to data oscillation.

Theorem 5 (quasi-best approximation up to data oscillation) *For any $p \in \mathbb{N}_0$, the solution u to (3) and the discrete solution u_h to (18) satisfy*

$$\begin{aligned}&|||u - Ru_h|||_{\mathrm{pw}} + s_h(u_h, u_h)^{1/2}\\ &\quad\le C_{12}\Big(\min_{v_{k+1}\in P_{k+1}(\mathcal{T})} |||u - v_{k+1}|||_{\mathrm{pw}} + \mathrm{osc}_{k+p}(f, \mathcal{T})\Big).\end{aligned}$$

The constant C_12 exclusively depends on k, p, and the shape regularity of $\mathcal{T}$.

Proof Given $k, p \in \mathbb{N}_0$, let $\widetilde{u} \in V$ solve the Poisson model problem $-\Delta\widetilde{u} = \Pi_{k+p}f$ with the right-hand side $\Pi_{k+p}f$. Section 4.3 in [32] constructs a stable enriching operator $\mathcal{J} : V_h \to V$ with local bubble-functions from [38]. A modification, where the polynomial degree $k-1$ in [32, Eq. (4.16)] is replaced by $k+p$, leads to a right-inverse $\mathcal{J} : V_h \to V$ of the interpolation $\mathrm{I} : V_h \to V$ with the stability $|||\mathcal{J}v_h|||^2 \lesssim a_h(v_h, v_h)$ and the additional L^2 orthogonality $\mathcal{J}v_h - v_{\mathcal{T}} \perp P_{k+p}(\mathcal{T})$ for all $v_h = (v_{\mathcal{T}}, v_{\mathcal{F}}) \in V_h$. The extra orthogonality allows for

$$(\Pi_{k+p}f, \mathcal{J}v_h)_{L^2(\Omega)} = (\Pi_{k+p}f, v_{\mathcal{T}})_{L^2(\Omega)} = (f, v_{\mathcal{T}})_{L^2(\Omega)} \quad \text{for all } (v_{\mathcal{T}}, v_{\mathcal{F}}) \in V_h.$$

Consequently, the smoother $\mathcal{J}$ leads to a discrete solution $u_h = (u_{\mathcal{T}}, u_{\mathcal{F}}) \in V_h$ in the modified HHO discretization of [32] as a quasi-best approximation of the above solution $\tilde{u}$. The point is that $u_h \in V_h$ coincides with the original HHO solution u_h from (18). The arguments from the proof of [32, Theorem 4.10] reveal the quasi-best approximation

$$|||\tilde{u} - Ru_h|||_{\mathrm{pw}} + s_h(u_h, u_h)^{1/2} \lesssim \min_{v_{k+1} \in P_{k+1}(\mathcal{T})} |||\tilde{u} - v_{k+1}|||_{\mathrm{pw}}$$

also for the above modified smoother $\mathcal{J}$. This, the triangle inequalities $|||u - Ru_h|||_{\mathrm{pw}} \leq |||u - \tilde{u}||| + |||\tilde{u} - Ru_h|||_{\mathrm{pw}}$ and $|||\tilde{u} - v_{k+1}|||_{\mathrm{pw}} \leq |||u - \tilde{u}||| + |||u - v_{k+1}|||_{\mathrm{pw}}$ for any $v_{k+1} \in P_{k+1}(\mathcal{T})$, and the standard perturbation bound $|||u - \tilde{u}||| \leq C_P \mathrm{osc}_{k+p}(f, \mathcal{T})$ conclude the proof. □

4.5 Stabilization-free efficiency of averaging

The main result of this subsection establishes the stabilization-free efficiency of the nodal averaging technique.

Theorem 6 (averaging is efficient) *Let $u \in V$ resp. $u_h \in V_h$ solve (3) resp. (18). Then Ru_h and $\mathcal{A}Ru_h$ satisfy, for any $p \in \mathbb{N}_0$, that*

$$C_{13}{}^{-1} |||(1 - \mathcal{A})Ru_h|||_{\mathrm{pw}} \leq |||u - Ru_h|||_{\mathrm{pw}} + \mathrm{osc}_{k+p}(f, \mathcal{T}). \tag{54}$$

The constant C_12 exclusively depends on k, p, and the shape regularity of the triangulation $\mathcal{T}$.

The proof can follow the proof of [25, Theorem 4.7] but additionally utilizes the two significant improvements from Sects. 4.3–4.4 that allow a stabilization-free efficiency in (54).

Proof Theorem 4.7 in [25] shows $|||(1 - \mathcal{A})Ru_h|||^2_{\mathrm{pw}} \lesssim |||u - Ru_h|||^2_{\mathrm{pw}} + \tilde{s}_h(u_h, u_h)$. This, the equivalence $\tilde{s}_h(u_h, u_h) \approx s_h(u_h, u_h)$ of stabilizations (from Theorem 4), and the efficiency $s_h(u_h, u_h) \lesssim |||u - Ru_h|||^2_{\mathrm{pw}} + \mathrm{osc}^2_{k+p}(f, \mathcal{T})$ (from Theorem 5) imply the assertion. □

Remark 2 (p-robustness) The $H^1(\Omega)$-conforming post-processing of Ru_h from [31] provides an efficiency constant independent of the polynomial degree k. The right-hand side of [31, Corollary 4.2] involves the stabilization-related term $\sum_{F \in \mathcal{F}} h_F^{-1} \|\Pi_{F,0}[Ru_h]_F\|^2_{L^2(F)}$. It remains an open question whether this term can be controlled p-robustly by $|||u - Ru_h|||_{\mathrm{pw}} + \mathrm{osc}_k(f, \mathcal{T})$ (with a multiplicative constant independent of the polynomial degree k).

4.6 Proof of Theorem 3

Let $p \in \mathbb{N}_0$ and $r = 0$ if $k = 0$ and $r = k + p$ if $k \geq 1$ as in (35) be given. Recall the abbreviation $G_h = \nabla_{\mathrm{pw}} Ru_h \in P_k(\mathcal{T})$ with the discrete solution $u_h \in V_h$ to (18) and

let $Q_p = \sum_{z\in\mathcal{V}} Q_{z,h} \in H(\mathrm{div},\Omega)$ denote the flux reconstruction from Sect. 4.2. The proof establishes (36) in five steps.

Step 1 provides the GUB $|||u - Ru_h|||_{\mathrm{pw}} \leq \eta_{\mathrm{eq},p}(\mathcal{T})$. This can follow from the paradigm of [1, 2, 30] as outlined below. The choice $G := G_h$ and $w := \mathcal{A}Ru_h$ in (8) and a triangle inequality lead to

$$|||u - Ru_h|||_{\mathrm{pw}}^2 \leq (|||f + \mathrm{div}\, Q_p|||_* + |||\mathrm{div}(Q_p - G_h)|||_*)^2 + |||(1-\mathcal{A})Ru_h|||_{\mathrm{pw}}^2.$$

Since $\mathrm{div}\, Q_p + \Pi_r f = 0$ vanishes in Ω by (42), a piecewise Poincaré inequality shows $|||f + \mathrm{div}\, Q_p|||_* \leq C_P \mathrm{osc}_r(f,\mathcal{T})$. This, the bound $|||\mathrm{div}(Q_p - G_h)|||_* \leq \|Q_p - G_h\|$ from the definition of $|||\bullet|||_*$, and the previously displayed formula result in the reliability $|||u - Ru_h|||_{\mathrm{pw}} \leq \eta_{\mathrm{eq,p}}(\mathcal{T})$.

Step 2 establishes $\mathrm{osc}_{k-1}(f,\mathcal{T}) \lesssim \eta_{\mathrm{eq},p}(\mathcal{T})$. Lemma 8 provides

$$\mathrm{osc}_{k-1}(f,\mathcal{T}) \lesssim |||u - Ru_h|||_{\mathrm{pw}} + \mathrm{osc}_r(f,\mathcal{T}). \tag{55}$$

This, Step 1 and $\mathrm{osc}_r(f,\mathcal{T}) \lesssim \eta_{\mathrm{eq},p}(\mathcal{T})$ from (34) conclude the proof of Step 2.

Step 3 reveals, for any $q \in \mathbb{N}_0$, the efficiency of the flux reconstruction

$$\|Q_p - G_h\| \lesssim |||u - Ru_h|||_{\mathrm{pw}} + \mathrm{osc}_q(\mathcal{T}, f) \tag{56}$$

for any polynomial degree $k \geq 1$. The case $k = 0$ follows in Step 4 below. Recall $f_z = \Pi_{k+p}(\varphi_z f - G_h \cdot \nabla\varphi_z)$ from (39) for any vertex $z \in \mathcal{V}$ in the construction of Q_p from Sect. 4.2 and set $\sigma_z := \mathcal{I}_{\mathrm{RT}}(\varphi_z G_h) \in RT_{k+p}^{\mathrm{pw}}(\mathcal{T}(z))$. The piecewise Raviart-Thomas interpolation $\mathcal{I}_{\mathrm{RT}} : H^1(\mathcal{T};\mathbb{R}^n) \to RT_{k+p}^{\mathrm{pw}}(\mathcal{T})$ satisfies the well-known commuting diagram properties [7, Section 2.5.1]

$$\mathrm{div}_{\mathrm{pw}} \circ \mathcal{I}_{\mathrm{RT}} = \Pi_{k+p} \circ \mathrm{div}_{\mathrm{pw}} \qquad \text{and} \qquad \gamma_T \circ \mathcal{I}_{\mathrm{RT}}|_F = \Pi_{F,k+p} \circ \gamma_T \tag{57}$$

for any facet $F \in \mathcal{F}(T)$ of a simplex $T \in \mathcal{T}$ and the normal trace $\gamma_T : H^1(T;\mathbb{R}^n) \to L^2(\partial T)$ with $\gamma_T\sigma := \sigma \cdot \nu_T$ for $\sigma \in H^1(T;\mathbb{R}^n)$. This and elementary algebra with the product rule $\mathrm{div}_{\mathrm{pw}}(\varphi_z G_h) = \varphi_z \mathrm{div}_{\mathrm{pw}} G_h + \nabla\varphi_z \cdot G_h \in P_k(\mathcal{T}(z))$ imply

$$r_z := -\mathrm{div}_{\mathrm{pw}}\sigma_z - f_z = -\varphi_z \mathrm{div}_{\mathrm{pw}} G_h - \Pi_{k+p}(\varphi_z f) \in P_{k+p}(\mathcal{T}(z)). \tag{58}$$

Recall the residual $\mathrm{Res}_z(v)$ with $v \in H^1(\Omega)$ for the vertex $z \in \mathcal{V}$ from (44). The commuting diagram property (57)–(58) establish the identity

$$\mathrm{Res}_z(1) = -(\mathrm{div}_{\mathrm{pw}} G_h + f, \varphi_z)_{L^2(\omega(z))} + \sum_{T\in\mathcal{T}(z)} \langle G_h \cdot \nu_T, \varphi_z\rangle_{L^2(\partial T)}.$$

This, a piecewise integration by parts, and the property (20) verify $\mathrm{Res}(1) = (G_h, \nabla\varphi_z)_{L^2(\omega(z))} - (f,\varphi_z)_{L^2(\omega(z))} = 0$ for any interior vertex $z \in \mathcal{V}(\Omega)$. Hence,

Lemma 9 applies for any vertex $z \in \mathcal{V}$ and provides

$$\|Q_{z,h} - \mathcal{I}_{RT}(\varphi_z G_h)\|_{L^2(\omega(z))} \leq C_{\mathrm{s}} \sup_{\substack{v \in H^1_*(\omega(z)) \\ \|\nabla v\|_{L^2(\omega(z))}=1}} \mathrm{Res}_z(v) \tag{59}$$

for the local contributions $Q_{z,h}$ of $Q_p = \sum_{z\in\mathcal{V}} Q_{z,h}$ from (41). The identity $\mathcal{I}_{\mathrm{RT}}(\varphi_z G_h) = \varphi_z G_h$ for $p \geq 1$ from $\varphi_z G_h \in P_{k+1}(\mathcal{T}(z)) \subset RT^{\mathrm{pw}}_{k+p}(\mathcal{T}(z))$ allows for a k- and p-robust efficiency control of the flux reconstruction error

$$C_{14}{}^{-1}\|Q_p - G_h\|^2 \leq \|\nabla u - G_h\|^2 + \sum_{z\in\mathcal{V}} \mathrm{osc}_r^2(\varphi_z f, \mathcal{T}(z)) \tag{60}$$

with a constant C_14 that solely depends on the shape regularity of $\mathcal{T}$. This is deemed noteworthy and motivates two different approaches for the bound of the residual $\mathrm{Res}_z(v)$ on the right-hand side of (59) for $p = 0$ and $p \geq 1$ below.

Step 3.1 provides (56) for $p = 0$. Given any normalized $v \in H^1_*(\omega(z))$ with $\|\nabla v\|_{L^2(\omega(z))} = 1$, the product $\mathcal{I}_{RT}(\varphi_z G_h) \cdot \nu_F\, v$ vanishes on any boundary facet $F \in \mathcal{F}(\partial\omega(z))$ of the patch $\omega(z)$. This, the commuting diagram property (57), and (58) with $\varphi_z \mathrm{div}_{\mathrm{pw}} G_h \in P_k(\mathcal{T}(z))$ in the definition of the residual $\mathrm{Res}_z(v)$ from (44) verify

$$\begin{aligned}\mathrm{Res}_z(v) = &-(\varphi_z f + \varphi_z \mathrm{div}_{\mathrm{pw}} G_h, \Pi_k v)_{L^2(\omega(z))} \\ &+ \sum_{F\in\mathcal{F}(z)\cap\mathcal{F}(\Omega)} \langle \varphi_z [G_h]_F \cdot \nu_F, \Pi_{F,k} v\rangle_{L^2(F)}.\end{aligned} \tag{61}$$

The shape regularity of $\mathcal{T}$, a Poincaré inequality for interior vertices $z \in \mathcal{V}(\Omega)$, and a Friechrichs inequality for boundary vertices $z \in \mathcal{V}(\partial\Omega)$ provide

$$\|h_{\mathcal{T}}^{-1} v\|_{L^2(\omega(z))} \approx \mathrm{diam}(\omega(z))^{-1}\|v\|_{L^2(\omega(z))} \lesssim \|\nabla v\|_{L^2(\omega(z))} = 1. \tag{62}$$

Given any facet $F \in \mathcal{F}(z) \cap \mathcal{F}(\Omega)$ in the facet spider $F \in \mathcal{F}(z)$ with facet patch $\omega(F)$, a trace inequality thus shows

$$h_F^{-1/2}\|v\|_{L^2(F)} \lesssim \|h_{\mathcal{T}}^{-1} v\|_{L^2(\omega(F))} + \|\nabla v\|_{L^2(\omega(F))} \lesssim 1. \tag{63}$$

Cauchy inequalities on the right-hand side of (61), the stability of the L^2 projection, $\|\varphi_z\|_{L^\infty(\omega_z)} = 1$, and (62)–(63) prove that $\mathrm{Res}_z(v)$ is controlled by

$$\|h_{\mathcal{T}}(f + \mathrm{div}_{\mathrm{pw}} G_h)\|_{L^2(\omega(z))} + \left(\sum_{F\in\mathcal{F}(z)\cap\mathcal{F}(\Omega)} h_F \|[G_h]_F \cdot \nu_F\|^2_{L^2(F)}\right)^{1/2}.$$

The efficiency of those residual terms follows from the proof of Theorem 2 in Sect. 3. In combination with (43) and (59), this results in the global efficiency (56) for $p = 0$ and concludes the proof of Step 3.1.

Step 3.2 provides (56) for $p \geq 1$. Given any normalized $v \in H^1_*(\omega(z))$ with $\|\nabla v\|_{L^2(\omega(z))} = 1$, (58) and the identity $\mathcal{I}_{\mathrm{RT}}(\varphi_z G_h) = \varphi_z G_h$ in the definition of the residual $\mathrm{Res}_z(v)$ from (44) verify that $\mathrm{Res}_z(v)$ is equal to

$$-(\varphi_z \mathrm{div}_{\mathrm{pw}} G_h + \Pi_{k+p}(\varphi_z f), v)_{L^2(\omega(z))} + \sum_{T \in \mathcal{T}(z)} \langle G_h \cdot \nu_T, \varphi_z v \rangle_{L^2(\partial T)}.$$

This, a piecewise integration by parts, and the product rule $\nabla(\varphi_z v) = \varphi_z \nabla v + v \nabla \varphi_z$ reveal

$$\mathrm{Res}_z(v) = -(\Pi_{k+p}(\varphi_z f), v)_{L^2(\omega(z))} + (G_h, \nabla(\varphi_z v))_{L^2(\omega(z))}. \tag{64}$$

The weak formulation (3) with the test function $\varphi_z v \in H^1_0(\omega(z)) \subset V$ shows $(\nabla u, \nabla(\varphi_z v))_{L^2(\omega(z))} = (f, \varphi_z v)_{L^2(\omega(z))}$. Consequently, (64) implies

$$\mathrm{Res}_z(v) = ((1 - \Pi_{k+p})(\varphi_z f), v)_{L^2(\omega(z))} - (\nabla u - G_h, \nabla(\varphi_z v))_{L^2(\omega(z))}.$$

This, a Cauchy-Schwarz, and a piecewise Poincaré inequality with the normalization $\|\nabla v\|_{L^2(\omega(z))} = 1$ provide

$$\mathrm{Res}_z(v) \leq \|\nabla u - G_h\|_{L^2(\omega(z))} \|\nabla(\varphi_z v)\|_{L^2(\omega(z))} + C_P \mathrm{osc}_{k+p}(\varphi_z f, \mathcal{T}(z)). \tag{65}$$

Since $\|\nabla \varphi_z\|_{L^\infty(\omega(z))} \approx h^{-1}$, the Leibniz rule, a triangle inequality, and (62) show that

$$\begin{aligned} \|\nabla(\varphi_z v)\|_{L^2(\omega(z))} &\leq \|\varphi_z\|_{L^\infty(\omega(z))} \|\nabla v\|_{L^2(\omega(z))} + \|\nabla \varphi_z\|_{L^\infty(\omega(z))} \|v\|_{L^2(\omega(z))} \\ &\lesssim \|\nabla v\|_{L^2(\omega(z))} = 1 \end{aligned}$$

can be bounded by a constant independent of h. Thus, the combination of (43) with (59) and (65) results in the efficiency of $\|Q_p - G_h\|$ in (60) with a k- and p-robust constant C_{14}. Since $\varphi_z \Pi_{k-1} f \in P_k(T) \subset P_{k+p}(T)$, the Pythagoras theorem and $\|\varphi_z\|_{L^\infty(\omega(z))} = 1$ show $\|(1 - \Pi_{k+p})(\varphi_z f)\|_{L^2(T)} \leq \|\varphi_z (1 - \Pi_{k-1}) f\|_{L^2(T)} \leq \|(1 - \Pi_{k-1}) f\|_{L^2(T)}$ for all $T \in \mathcal{T}(z)$, whence

$$\mathrm{osc}_{k+p}(\varphi_z f, \mathcal{T}(z)) \leq \mathrm{osc}_{k-1}(f, \mathcal{T}(z)).$$

This and Lemma 8 implies the efficiency

$$\mathrm{osc}_{k+p}(\varphi_z f, \mathcal{T}(z)) \lesssim \|\nabla_{\mathrm{pw}}(u - Ru_h)\|_{L^2(\omega(z))} + \mathrm{osc}_q(f, \mathcal{T}(z))$$

of the local oscillations from (65) for any $q \in \mathbb{N}_0$ as in Remark 1. This and (60) prove (56) for $p \geq 1$ and conclude the proof of Step 3.2.

Step 4 affirms the efficiency of the flux reconstruction

$$C_{15}^{-1}\|Q_p - G_h\| \leq |||u - Ru_h|||_{\mathrm{pw}} + \mathrm{osc}_q(f, \mathcal{T}) \tag{66}$$

for the polynomial degree $k = 0$ and any $q \in \mathbb{N}_0$. Let $\widetilde{u} \in V$ solve the Poisson model problem $-\Delta\widetilde{u} = \Pi_0 f$ with piecewise constant right-hand side $\Pi_0 f \in P_0(\mathcal{T})$. A careful inspection reveals that all arguments from Step 3 apply to the case $k = 0$ for f replaced by $\Pi_0 f$. This leads to $\|Q_p - G_h\| \leq C_{15}|||\widetilde{u} - Ru_h|||_{\mathrm{pw}}$ with a constant C_{15} that solely depends on the shape of $\mathcal{T}$ (because the data oscillations on the right-hand side of (60) vanish). Therefore, the triangle inequality $|||\widetilde{u} - Ru_h|||_{\mathrm{pw}} \leq |||u - \widetilde{u}||| + |||u - Ru_h|||_{\mathrm{pw}}$, the standard bound $|||u - \widetilde{u}||| \leq C_P\mathrm{osc}_0(f, \mathcal{T})$, and $C_P = 1/\pi < 1$ on simplicial domains lead to (66). This and the efficiency of the data oscillations from Lemma 8 conclude the proof of Step 4. Notice that the constant C_{15} is independent of the parameter p.

Step 5 finishes the proof. On the one hand, the reliability $|||u - Ru_h|||_{\mathrm{pw}} + \mathrm{osc}_{k-1}(f, \mathcal{T}) \lesssim \eta_{\mathrm{eq},p}$ is established in Step 1–2. On the other hand, the efficiency of the averaging operator from Theorem 6, Lemma 8, and the efficiency of the flux reconstruction in (56) for $k \geq 1$ and in (66) for $k = 0$ imply the efficiency $\eta_{\mathrm{eq,p}} \lesssim |||u - Ru_h|||_{\mathrm{pw}} + \mathrm{osc}_q(f, \mathcal{T})$ for any $q \in \mathbb{N}_0$. This concludes the proof of Theorem 3.

5 Numerical experiments

This section provides numerical evidence for optimal convergence and a comparison of the stabilization-free GUBs η_{res} and $\eta_{\mathrm{eq,p}}$ from the Sects. 3 and 4 with the original error estimator η_{HHO} from [25, Theorem 4.3] for the HHO method in three 2D benchmarks.

5.1 A posteriori error estimation with explicit constants

All triangulations in this section consist of right-isosceles triangles with the Poincaré constant $C_P = (\sqrt{2}\pi)^{-1}$ [34]. With the estimates $C_1 \leq C_{\mathcal{T}}$, $C_{\mathrm{H}} \leq 1$, and $C_2 \leq C_{\mathcal{F}}$ from Example 1, the residual-based error estimator from (22) reads

$$\eta_{\mathrm{res}}^2(\mathcal{T}) := \big(C_{\mathcal{T}}\eta_{\mathrm{res},1}(\mathcal{T}) + C_P\eta_{\mathrm{res},2}(\mathcal{T}) + C_{\mathcal{F}}\eta_{\mathrm{res},3}(\mathcal{T})\big)^2 + C_{\mathcal{F}}^2\eta_{\mathrm{res},4}^2(\mathcal{T}).$$

The equilibrated GUB from Theorem 3,

$$\eta_{\mathrm{eq},p}^2(\mathcal{T}) := \Big(C_P\mathrm{osc}_{k+p}(f, \mathcal{T}) + \|Q_p^{\Delta}\|_{L^2(\Omega)}\Big)^2 + |||(1 - \mathcal{A})Ru_h|||_{\mathrm{pw}}^2,$$

depends on the post-processed quantity $Q_p^{\Delta} := Q_p - \nabla_{\mathrm{pw}}Ru_h$ with the Raviart-Thomas function $Q_p \in RT_{k+p}(\mathcal{T})$ of degree $k + p$ for $p \in \mathbb{N}_0$ from Sect. 4.2. An algorithmic description of the computation of Q_p^{Δ} for arbitrary p follows in Appendix A. Theorem 3 shows that $\eta_{\mathrm{eq},p}$ is efficient and reliable for all $p \in \mathbb{N}_0$. The residual-

based error estimator η_{HHO} from [25, Theorem 4.3] reads

$$\eta_{\mathrm{HHO}}^2(\mathcal{T}) := \sum_{T\in\mathcal{T}} \Bigg(C_P h_T \|(I-\Pi_{T,0})(f+\Delta_{\mathrm{pw}} R u_h)\|_{L^2(T)} + \sqrt{\sum_{F\in\mathcal{F}(T)} C_{\partial T} h_T \|R_{T,F}^k u_h\|_{L^2(F)}^2} \Bigg)^2 + |||(I-\mathcal{A})Ru_h|||_{\mathrm{pw}}^2$$

with the operator $R_{T,F}^k$ from [25, Eq. (2.59)] for the original HHO stabilization [25, Eq. (2.22)] that induces the global stabilization s_h. The constant $C_{\partial T} = 12C_P(C_P + C_{\mathrm{tr}}) \leq 2.0315$ for right-isosceles triangles bounds the trace of $f-\Pi_0 f$ for $f \in H^1(T)$ and improves on the estimate $C_{\partial T} \leq (C_P(h_T|\partial T|/|T|)(1+C_P))^2 = 2.524$ from [25, Subs. 4.1.1].

Lemma 10 (Poincaré-type inequality on trace) *Given a simplex $T \subset \mathbb{R}^n$, any $f \in H^1(T)$ and $C_{\partial T} := (n+1)h_T^2|T|^{-1}C_P(C_P + 2C_{\mathrm{tr}}/n)$ satisfy*

$$\|f-\Pi_0 f\|_{L^2(\partial T)}^2 \leq C_{\partial T} h_T \|\nabla f\|_{L^2(T)}^2. \tag{67}$$

Proof Abbreviate $\tilde{\ell}(F) := (n+1)h_F h_T^2 |T|^{-1}$ for the facet $F \in \mathcal{F}(T)$ of T and apply Lemma 3 to the singleton triangulation $\{T\}$ and $f - \Pi_0 f \in H^1(T)$. This and the Poincaré inequality $\|f-\Pi_{0,T} f\|_{L^2(T)} \leq C_P h_T \|\nabla f\|_{L^2(T)}$ show

$$\sum_{F\in\mathcal{F}(T)} \tilde{\ell}(F)^{-1} \|f-\Pi_{0,T} f\|_{L^2(F)}^2 \leq (C_P + 2C_{\mathrm{tr}}/n) C_P \|\nabla f\|_{L^2(T)}^2.$$

The assertion (67) follows from the observation that $\tilde{\ell}(F)$ is maximized on the facet $F \in \mathcal{F}(T)$ with $h_F = h_T$. □

5.2 Implementation and adaptive algorithm

Our implementation of the HHO method in MATLAB uses nodal bases for the spaces $P_k(\mathcal{F})$, $P_k(\mathcal{T})$, and $P_{k+1}(\mathcal{T})$ and the direct solver *mldivide* (behind the \-operator) for the discrete system of equations representing (18). For implementation details on the HHO method itself we refer to [25, Appendix B]. The integration of polynomial expressions is carried out exactly. The errors in approximating non-polynomial expressions, such as exact solutions u and source terms f, by polynomials of sufficiently high degree are expected to be very small and are neglected for simplicity.

Algorithm 1 displays the standard adaptive algorithm (AFEM) [16, 22] driven by the refinement indicators, for any triangle $T \in \mathcal{T}$,

$$\eta_{\mathrm{res}}^2(T) := |T|\|f+\Delta_{\mathrm{pw}} R u_h\|_{L^2(T)}^2 + |T|^{1/2} \sum_{F\in\mathcal{F}(T)} \|[\nabla_{\mathrm{pw}} R u_h]_F\|_{L^2(F)}^2 \tag{68}$$

with the modified jump $[\bullet]_F := \bullet \times n_F$ along a boundary side $F \in \mathcal{F}(\partial\Omega)$ and the newest-vertex-bisection (NVB). The sum of this over all triangles is, up to some multiplicative constants, equivalent to $\eta_{\mathrm{res}}^2(\mathcal{T})$.

Algorithm 1 AFEM algorithm

Input: Initial regular triangulation $\mathcal{T}_0$ and polynomial degree $k \in \mathbb{N}_0$ of the HHO method
for levels $\ell := 0, 1, 2...$ **do**
Solve (18) for discrete solution $u_\ell \in V_\ell$ exactly on $\mathcal{T}_\ell$ and compute Ru_ℓ
Compute (refinement indicators) $\eta_{\mathrm{res}}^2(T)$ for all $T \in \mathcal{T}_\ell$
Mark minimal subset $\mathcal{M}_\ell \subset \mathcal{T}_\ell$ with $\frac{1}{2}\sum_{T\in\mathcal{T}_\ell} \eta_{\mathrm{res}}^2(T) \le \sum_{T\in\mathcal{M}_\ell} \eta_{\mathrm{res}}^2(T)$
Refine $\mathcal{T}_\ell$ to smallest NVB refinement $\mathcal{T}_{\ell+1}$ with $\mathcal{M}_\ell \subseteq \mathcal{T}_\ell \setminus \mathcal{T}_{\ell+1}$
end for
Output: sequences of triangulations $\mathcal{T}_\ell$ and Ru_ℓ

5.3 High oscillations on the unit square

This benchmark on the unit square $\Omega := (0, 1)^2$ considers the Laplace equation $-\Delta u = f$ with source term f matching the smooth exact solution

$$u(x, y) = x(x-1)y(y-1)e^{-100((x-1/2)^2+(y-117/1000)^2)} \in C^\infty(\Omega).$$

Figure 1 displays the energy norm $|||e|||_{\mathrm{pw}}$ of the error $e := u - Ru_h$ for uniform and adaptive refinement by Algorithm 1 on the left. The smooth solution allows for optimal convergence rates $(k+1)/2$ in the number ndof of degrees of freedom, while the adaptive mesh sequence leads to a lower energy error with respect to ndof. The GUBs η_{res}, $\eta_{\mathrm{eq},p}$, and η_{HHO} are efficient and therefore equivalent to the energy error $|||e|||_{\mathrm{pw}}$, see Fig. 1 on the right for $k = 0, 2$.

Figure 2 shows the efficiency indices $EF(\eta) := \eta/|||e|||_{\mathrm{pw}}$ for the residual-based GUBs $\eta = \eta_{\mathrm{res}}, \eta_{\mathrm{HHO}}$ and the equilibration-based GUB $\eta = \eta_{\mathrm{eq},p}$ for $p = 0, 1$. Higher values of p for a more expensive postprocessing in $\eta_{\mathrm{eq},p}$ do not significantly improve on $\eta_{\mathrm{eq},1}$.

5.4 Analytical solution for the slit domain

The source term $f \in L^2(\Omega)$ in the second benchmark on the slit domain $\Omega := (0, 1)^2 \setminus ([0, 1) \times \{0\})$ matches the singular solution (in polar coordinates)

$$u(r, \varphi) = r^{1/2}(r^2 \sin(\varphi)^2 - 1)(r^2 \cos(\varphi)^2 - 1)\sin(\varphi/2).$$

The singularity of u at the origin $(0, 0)$ leads to reduced convergence rates $1/4$ under uniform refinement, regardless of the polynomial degree k. Figure 3 shows that the adaptive algorithm recovers optimal rates and verifies the equivalence of the GUBs η_{res}, $\eta_{\mathrm{eq},p}$, and η_{HHO} to the energy error $|||e|||_{\mathrm{pw}}$.

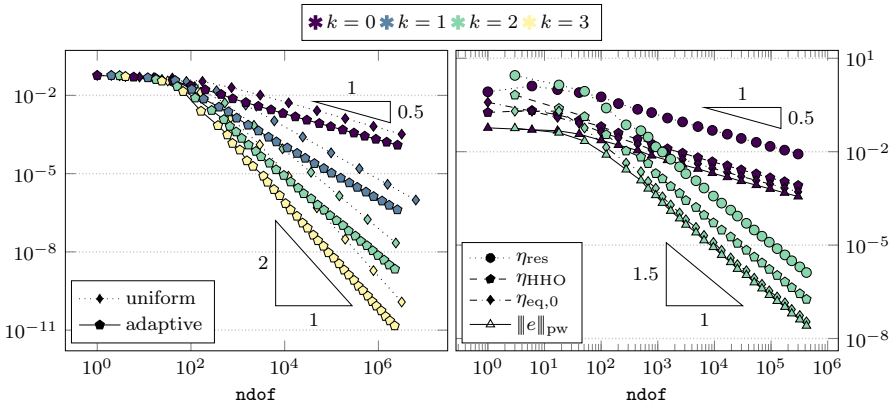

Fig. 1 Convergence history of the energy error $|||e|||_{\mathrm{pw}}$ (left) and the GUBs η_{res}, η_{HHO}, $\eta_{\mathrm{eq},0}$ (right) on the square domain

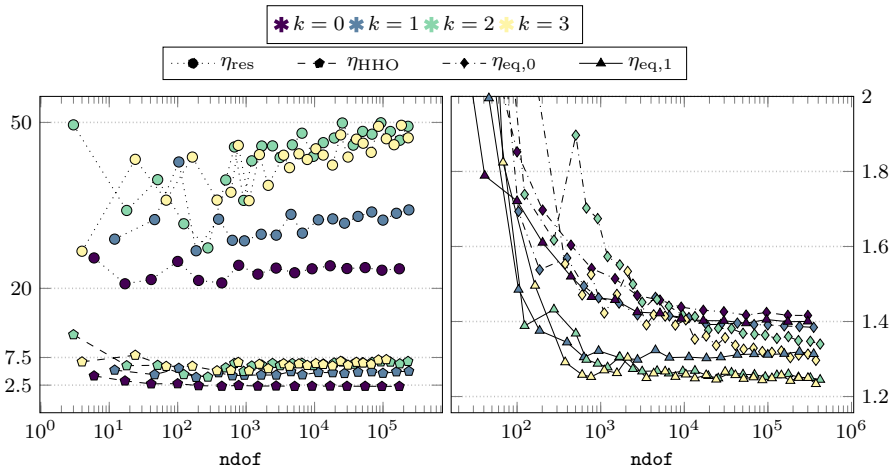

Fig. 2 History of the overestimation factor $EF(\eta) = \eta/|||e|||_{\mathrm{pw}}$ for the residual-based error estimators η_{res}, η_{HHO} (left) and $\eta_{\mathrm{eq},0}$, $\eta_{\mathrm{eq},1}$ (right) on the unit square

The efficiency indices in Fig. 4 show a strong overestimaton by η_{res} in the preasymptotic regime (undisplayed) with values $EF(\eta_{\mathrm{res}}) > 60$. However, asymptotically the quotients $EF(\eta) = \eta/|||e|||_{\mathrm{pw}}$ for the two residual-based GUBs η_{res}, η_{HHO} differ only by a factor 10, while the equilibrated GUBs $\eta_{\mathrm{eq},p}$ provide the closest values to 1.

5.5 Corner singularity in the L-shaped domain

The third benchmark problem is set in the L-shaped domain $\Omega = (-1,1)^2 \setminus [0,1)^2$ with constant right-hand side $f \equiv 1$ with an exact solution $u \in H^{1+s}(\Omega)$ for all $0 \leq s < 2/3$ [24, Theorem 14.6]. Figure 5 displays the convergence history of the

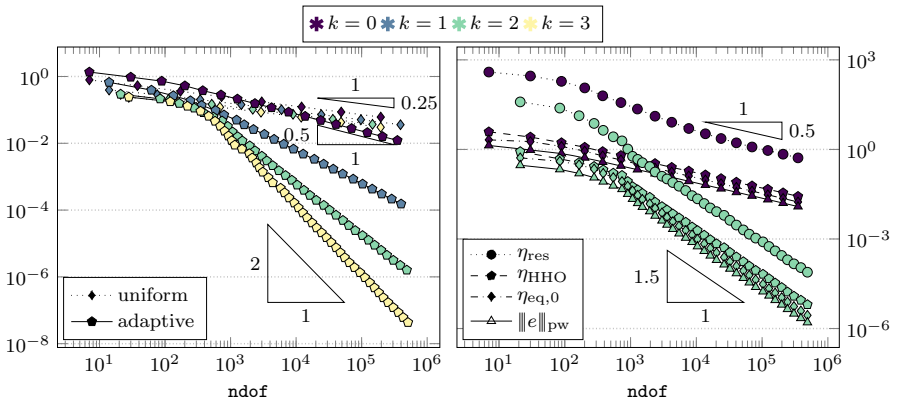

Fig. 3 Convergence history of the energy error $|||e|||_{\mathrm{pw}}$ (left) and the GUBs η_{res}, η_{HHO}, $\eta_{\mathrm{eq},0}$ (right) on the slit domain

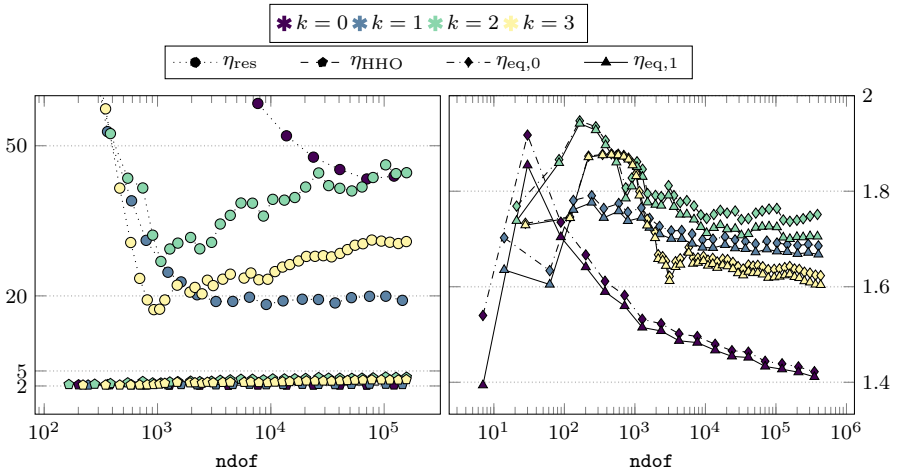

Fig. 4 History of the overestimation factor $EF(\eta) = \eta/|||e|||_{\mathrm{pw}}$ for the residual-based error estimators η_{res}, η_{HHO} (left) and $\eta_{\mathrm{eq},0}$, $\eta_{\mathrm{eq},1}$ (right) on the slit domain

error $e := u - Ru_h$ and compares the adaptive scheme, Algorithm 1, driven by the refinement indicators $\eta_{\mathrm{res}}(T)$ from (68) and

$$\eta^2_{\mathrm{HHO}}(T) := |T|\|(I-\Pi_0)(f+\Delta_{\mathrm{pw}}Ru_h)\|^2_{L^2(T)} + \|\nabla(1-\mathcal{A})Ru_h\|^2_{L^2(T)} + |T|^{1/2}\sum_{F\in\mathcal{F}(T)}\|R^k_{T,F}u_h\|^2_{L^2(F)},$$

$$\eta^2_{\mathrm{eq},0}(T) := \mathrm{osc}^2_k(f,T) + \|Q^{\Delta}_0\|^2_{L^2(T)} + \|\nabla(1-\mathcal{A})Ru_h\|^2_{L^2(T)}$$

for $T \in \mathcal{T}$ that are induced from the GUB η_{res}, η_{HHO}, and $\eta_{\mathrm{eq},0}$. Here, the norm $|||e|||_{\mathrm{pw}}$ of the distance e from the discrete solution $Ru_h \in P_{k+1}(\mathcal{T})$ over $\mathcal{T}$ to the unknown solution $u \in H^1(\Omega)$ is approximated by $|||\widehat{u} - Ru_h|||_{\mathrm{pw}}$, where $\widehat{u} \in P_{k+1}(\widehat{\mathcal{T}})$ is the

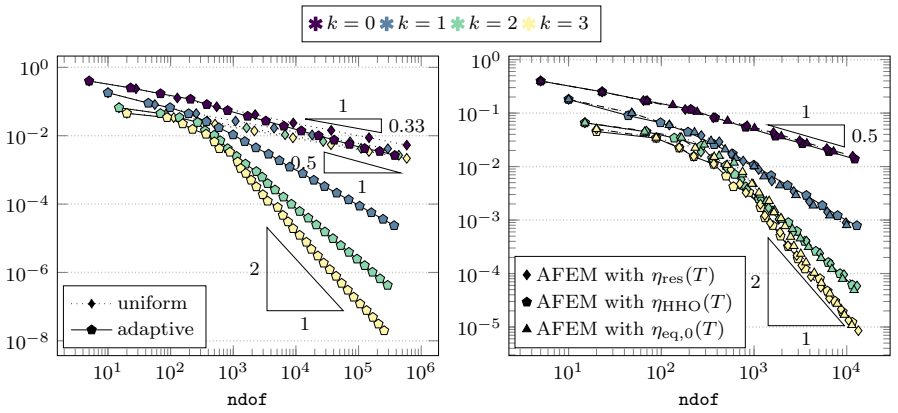

Fig. 5 Convergence history plot of the energy error $|||e|||_{\mathrm{pw}}$ on the L-shaped domain with uniform and adaptive refinement with AFEM, driven by $\eta_{\mathrm{res}}(T)$, (left) and for AFEM, driven by $\eta_{\mathrm{res}}(T)$, $\eta_{\mathrm{HHO}}(T)$, and $\eta_{\mathrm{eq},0}(T)$, (right)

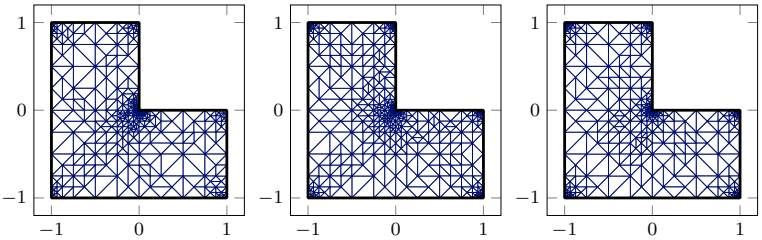

Fig. 6 Adaptive triangulations on the L-shaped domain for $k = 3$ from AFEM, driven by $\eta_{\mathrm{res}}(T)$ (left, $|\mathcal{T}| = 882$), driven by $\eta_{\mathrm{HHO}}(T)$ (middle, $|\mathcal{T}| = 907$), and driven by $\eta_{\mathrm{eq},0}(T)$ (right, $|\mathcal{T}| = 919$)

HHO approximation of u on an adaptive refinement $\widehat{\mathcal{T}}$ of $\mathcal{T}$ with at least $2|\mathcal{T}| \leq |\widehat{\mathcal{T}}|$ elements. The three adaptive schemes (Algorithm 1, driven by $\eta_{\mathrm{res}}(T)$, $\eta_{\mathrm{HHO}}(T)$, or $\eta_{\mathrm{eq},0}(T)$) recover optimal rates of convergence and lead to similar local refinement of the adaptive mesh sequences as in Fig. 6.

5.6 Conclusion

The adaptive mesh-refining algorithm recovers optimal convergence rates in all three benchmarks. This holds for AFEM driven by any of the three refinement indicators derived from the GUB η_{res}, η_{HHO}, and $\eta_{\mathrm{eq},p}$. The generated mesh sequences from the adaptive schemes, driven by the different estimators, display a very similar concentration of the local mesh-refinement as in Fig. 6. All three benchmarks verify that the considered error estimators are GUB with reliability constant 1, while the post-processing in the equilibrated GUB $\eta_{\mathrm{eq},p}$ produces minimal overestimation with significant additional computational costs.

Funding Open Access funding enabled and organized by Projekt DEAL.

Appendix A: Equilibration algorithm for higher order

The post-processed quantity $Q_p \in RT_{k+p}(\mathcal{T})$ from Sect. 4.2 enters the equilibrated error estimator $\eta_{\mathrm{eq},p}(\mathcal{T})$ in Theorem 3 and could be computed by a minimization problem on the vertex patches. The solution property (20) gives rise to the two cases $r = 0$ if $k = 0$ and $r = k + p$ if $k \geq 1$ for the polynomial degree r in the equilibrium $\operatorname{div} Q_p + \Pi_r f = 0$ in Ω from (42). This appendix follows [6, 9, 12, 37] to compute the quantity of interest $Q_p - \nabla_{\mathrm{pw}} R u_h$ directly in an efficient two-step procedure in 2D. Throughout this appendix, fix $k, p \in \mathbb{N}_0$ and abbreviate $q := k + p$ and $G_h := \nabla_{\mathrm{pw}} R u_h \in P_k(\mathcal{T}; \mathbb{R}^2)$. Let the data $f \in L^2(\Omega)$ be given and assume, for the sake of brevity, that $f \in P_0(\mathcal{T})$ if $k = 0$.

A.1 Overview

Recall the definition (41) of the summand $Q_{z,h}$ in $Q_p := \sum_{z \in \mathcal{V}} Q_{z,h}$ from Sect. 4.2 with the piecewise Raviart-Thomas interpolation $\mathcal{I}_{\mathrm{RT}} : H^1(\mathcal{T}; \mathbb{R}^2) \to RT_q^{\mathrm{pw}}(\mathcal{T})$ [7, Section III.3.1]. The focus is on one vertex $z \in \mathcal{V}$ with vertex-patch $\omega(z)$ and its triangulation $\mathcal{T}(z) = \{T \in \mathcal{T} \mid z \in T\}$. Consider set of edges $\mathcal{F}$ and the facet-spider $\mathcal{F}(z) = \{E \in \mathcal{F} \mid z \in E\}$ as in Fig. 7. The nodal basis function $\varphi_z \in S^1(\mathcal{T}(z))$ gives rise to the discrete spaces

$$RT_q^{\mathrm{pw},0}(\mathcal{T}(z)) := \{\sigma_z \in RT_q^{\mathrm{pw}}(\mathcal{T}(z)) \,:\, \sigma_z \cdot \nu_E = 0 \text{ for all } E \in \mathcal{F} \backslash \mathcal{F}(z)\},$$

$$\mathcal{S}(z) := \left\{ \sigma_z \in RT_q^{\mathrm{pw},0}(z) \,:\, \begin{array}{ll} \operatorname{div} \sigma_z & = -\Pi_{T,q}(\varphi_z (f + \operatorname{div} G_h)) \quad \text{for all } T \in \mathcal{T}(z) \\ [\sigma_z \cdot \nu_E]_E & = -\Pi_{E,q}(\varphi_z [G_h \cdot \nu_E]_E) \quad \text{for all } E \in \mathcal{F}(\omega(z)) \end{array} \right\}.$$

Proposition 1 (alternative minimization) *It holds*

$$Q_{z,h}^{\Delta} := Q_{z,h} - \mathcal{I}_{\mathrm{RT}}(\varphi_z G_h) = \operatorname*{arg\,min}_{\sigma_z \in \mathcal{S}(z)} \|\sigma_z\|_{L^2(\omega(z))}. \tag{69}$$

Proof Recall $f_z = \Pi_{\tilde{p}}(\varphi_z f - G_h \cdot \nabla \varphi_z)$ from (39). (Notice that this formula coincide with the definition (39) for $k = 0$ because $f \in P_0(\mathcal{T})$.) Given any $\sigma_z \in \mathcal{S}(z)$, the commuting diagram property $\operatorname{div}_{\mathrm{pw}} \circ \mathcal{I}_{\mathrm{RT}} = \Pi_q \circ \operatorname{div}_{\mathrm{pw}}$ [7, Proposition 2.5.2] shows

$$\operatorname{div}_{\mathrm{pw}}(\sigma_z + \mathcal{I}_{RT}(\varphi_z G_h)) = \operatorname{div}_{\mathrm{pw}} \sigma_z + \Pi_{\tilde{p}} \operatorname{div}_{\mathrm{pw}}(\varphi_z G_h) = -f_z. \tag{70}$$

By design of the interpolation $\mathcal{I}_{RT}$, $(\mathcal{I}_{RT}(\varphi_z G_h)_{|T} \cdot \nu_E)_{|E} = \Pi_{E,q}(\varphi_z G_h)_{|T} \cdot \nu_E$ holds and so $[\mathcal{I}_{\mathrm{RT}}(\varphi_z G_h) \cdot \nu_E]_E = \Pi_{E,q}(\varphi_z [G_h \cdot \nu_E]_E)$ follows for any $E \in \mathcal{F}(T)$ and $T \in$

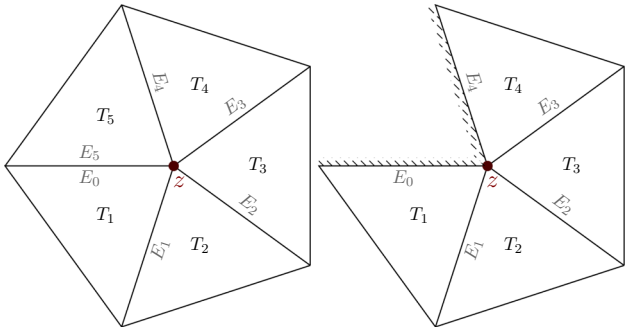

Fig. 7 Triangulation $\mathcal{T}(z)$ and enumeration of the edges $\mathcal{F}(z)$ of the vertex-patch $\omega(z)$ for an internal vertex $z \in \mathcal{V}(\Omega)$ with $N = |\mathcal{T}(z)| = 5$ (left) or boundary vertex $z \in \mathcal{V}(\partial\Omega)$ with $N = |\mathcal{T}(z)| = 4$ (right)

$\mathcal{T}$. Therefore, the jump $[\sigma_z + \mathcal{I}_{\mathrm{RT}}(\varphi_z G_h)]_E \cdot \nu_E \equiv 0$ vanishes on $E \in \mathcal{F}(\omega(z))$, whence $\sigma_z + \mathcal{I}_{\mathrm{RT}}(\varphi_z G_h) \in RT_{\tilde{p}}(\mathcal{T}(z))$. Since $RT_{\tilde{p}}^{\mathrm{pw},0}(\mathcal{T}(z)) \cap H(\mathrm{div}, \omega(z)) = RT_{\tilde{p}}^{0}(\mathcal{T}(z))$, this and (70) imply $\sigma_z + \mathcal{I}_{\mathrm{RT}}(\varphi_z G_h) \in \mathcal{Q}_h(z)$ for any $\sigma_z \in \mathcal{S}(z)$. In particular, $\mathcal{S}(z) + \mathcal{I}_{\mathrm{RT}}(\varphi_z G_h) \subseteq \mathcal{Q}_h(z)$. On the other hand, similar arguments verify the reverse inclusion $\mathcal{Q}_h(z) \subseteq \mathcal{S}(z) + \mathcal{I}_{\mathrm{RT}}(\varphi_z G_h)$. The substitution $\mathcal{S}(z) + \mathcal{I}_{\mathrm{RT}}(\varphi_z G_h) = \mathcal{Q}_h(z)$ in (41) concludes the proof. □

This establishes that the norm $\|Q_p^\Delta\|$ of $Q_p^\Delta := \sum_{z \in \mathcal{V}} Q_{z,h}^\Delta = Q_p - G_h$ contributes to the equilibrated error estimator and the remaining parts of this appendix compute the minimizer $Q_{z,h}^\Delta$ of (69) in a two-step procedure.

First, Algorithm 2 generates the coefficients of a particular solution $\tilde{\sigma}_z^\Delta \in \mathcal{S}(z)$ in terms of the finite element basis $\mathcal{B}_{RT}$ of $RT_q^{\mathrm{pw}}(\mathcal{T}(z))$ from Subsection A.2. The second step computes the correction

$$\sigma_z^\Delta := Q_{z,h}^\Delta - \tilde{\sigma}_z^\Delta = \operatorname*{arg\,min}_{\sigma_z \in V(z)} \|\sigma_z + \tilde{\sigma}_z^\Delta\|_{L^2(\omega(z))} \tag{71}$$

in terms of the low-dimensional unconstrained minimization problem over the linear space $V(z) := \mathcal{S}(z) - \tilde{\sigma}_z^\Delta = RT_q^{\mathrm{pw}}(\mathcal{T}(z)) \cap H(\mathrm{div} = 0, \omega(z))$ characterized in Lemma 12. Because [12, Lemma 3.1] is wrong (take, e.g., $\tau_K = \mathrm{curl}\, b_K \neq 0$ for the element bubble function b_K in their notation to see that uniqueness for general polynomial degrees q cannot hold) and [12] omits algorithmic details, this appendix focuses on the explicit characterization of the degrees of freedom for the minimization problem (71) over $V(z)$.

A.2 Degrees of freedom for $RT_q^{\mathrm{pw}}(T)$

This subsection introduces a basis for the Raviart-Thomas finite element on $T \in \mathcal{T}(z)$ and starts with the definition of some linear functionals on $H(\mathrm{div}, \mathcal{T})$. For any $\sigma \in$

$H(\mathrm{div}, \mathcal{T})$, set

$$\lambda^{\ell,m}_{T,\alpha}(\sigma) := \int_T \sigma \cdot e_\alpha \, x_1^\ell x_2^m \mathrm{d}x \qquad 0 \le \ell + m \le q-1, \alpha = 1, 2,$$
$$\lambda^{\ell,m}_{T,\mathrm{div}}(\sigma) := \int_T \mathrm{div}\, \sigma \, x_1^\ell x_2^m \mathrm{d}x \qquad 0 \le \ell + m \le q,$$
$$\lambda^{j}_{T,E}(\sigma) := \int_E \sigma_{|T} \cdot \nu_T \, s^j \mathrm{d}s \qquad 0 \le j \le q, E \in \mathcal{F}(T).$$

Here and throughout, $e_1 = (1, 0)$ and $e_2 = (0, 1)$ denote the canonical unit vectors in $\mathbb{R}^2$. Note that the (classical) degrees of freedom for the Raviart-Thomas finite element $RT_q(T)$ of degree $q \in \mathbb{N}_0$ from [11] read

$$\widetilde{\Lambda_T} := \{\lambda^j_{T,E}, \lambda^{\ell,m}_{T,\alpha} \text{ for } 0 \le j \le q, 0 \le \ell + m \le q-1, \alpha = 1, 2, E \in \mathcal{F}(T)\}.$$

This appendix requires, for the construction of $\tilde{\sigma}_z^\Delta \in \mathcal{S}(z)$, a different set of (unisolvent) degrees of freedom Λ_T for $RT_q(T)$ that includes the edge and divergence moments

$$\Lambda_T^0 := \{\lambda^j_{T,E}, \lambda^{\ell,m}_{T,\mathrm{div}} : \text{ for } 0 \le j \le q, 1 \le \ell + m \le q, E \in \mathcal{F}(T)\} \subseteq \Lambda_T. \quad (72)$$

(The set Λ_T^0 itself is linear independent [37, Lemma 3.1].) Given any Λ_T with (72), denote the remaining $N_q = q(q-1)/2$ degrees of freedom $\Lambda_T \setminus \Lambda_T^0$ by λ_T^r for $r = 1, \ldots, N_q$. Let $\mathcal{B}_{RT,T} = \{\varphi^j_{T,E}, \varphi^{\ell,m}_{T,\mathrm{div}}, \varphi^r_T\}$ be the unique basis of $RT_q(T)$ dual to Λ_T with inferred indices from Λ_T. Then, the collection $\mathcal{B}_{RT} := \bigcup_{T\in\mathcal{T}(z)} \mathcal{B}_{RT,T}$ is a basis of $RT_q^{\mathrm{pw}}(\mathcal{T}(z))$ and any function $\sigma_z \in RT_q^{\mathrm{pw}}(\mathcal{T}(z))$ has the representation

$$\sigma_z := \sum_{T\in\mathcal{T}(z)} \left(\sum_{E\in\mathcal{F}(T)} \sum_{j=0}^{q} c^j_{T,E} \varphi^j_{T,E} + \sum_{1\le\ell+m\le q} c^{\ell,m}_{T,\mathrm{div}} \varphi^{\ell,m}_{T,\mathrm{div}} + \sum_{r=1}^{N_q} c^r_T \varphi^r_T \right) \quad (73)$$

with coefficients $c^j_{T,E} = \lambda^j_{T,E}(\sigma_z)$, $c^{\ell,m}_{T,\mathrm{div}} = \lambda^{\ell,m}_{T,\mathrm{div}}(\sigma_z)$, and $c^r_T = \lambda^r_T(\sigma_z)$ for all $T \in \mathcal{T}(z)$, $E \in \mathcal{F}(T)$, and $0 \le j \le q$, $1 \le \ell + m \le q$, $1 \le r \le N_q$. By duality, the coefficients $c^j_{T,E}$ with $0 \le j \le q$ uniquely determine the normal trace $(\sigma_{z|T})_{|E} \cdot \nu_E \in P_q(E)$ on the edge $E \in \mathcal{F}(T)$ of $T \in \mathcal{T}(z)$. Any set of degrees of freedom Λ_T with (72) works with the equilibration algorithm in A.3.

Example 3 (Construction of Λ_T) This example presents a generic procedure to obtain such a set from $\widetilde{\Lambda_T}$. The integration by parts formula shows that the lowest-order divergence moment $\lambda^{0,0}_{T,\mathrm{div}} = \sum_{E\in\mathcal{F}(T)} \lambda^0_{T,E}$ depends linearly on the lowest-order edge moments and, similarly, the sums

$$\lambda^{\ell,m}_{T,\mathrm{div}} + \ell\lambda^{\ell-1,m}_{T,1} + m\lambda^{\ell,m-1}_{T,2} \in (P_{\ell+m}(\mathcal{F}(T)))^* \quad (74)$$

are functionals on $P_{\ell+m}(\mathcal{F}(T))$ (summands with negative indices are understood as zero). This relation allows for the substitution of volume moments in $\widetilde{\Lambda}_T$ for divergence moments $\lambda_{T,\mathrm{div}}^{\ell,m}$, $1 \leq \ell + m \leq q$, and leads to Λ_T with (72). The remaining degrees of freedom $\Lambda_T \setminus \Lambda_T^0$ are volume moments of the form $\lambda_T^r = \lambda_{T,\alpha}^{\ell,m}$ for a fixed $\alpha \in \{1, 2\}$, e.g.,

$$\Lambda_T \setminus \Lambda_T^0 = \{\lambda_{T,2}^{\ell,m} \;\; 1 \leq \ell \leq q-1, 0 \leq m \leq q-1-\ell\}.$$

A.3 Equilibration algorithm

Algorithm 2 Particular solution in $\mathcal{S}(z)$

Input: Data $f \in L^2(\omega(z))$ and $G_h \in H^1(\mathcal{T}(z))^2$ for vertex $z \in \mathcal{V}$.

1: Initialize all coefficients $c_{T,E}^j$, $c_{T,\mathrm{div}}^{\ell,m}$, c_T^r in (73) with zero.
2: **for** $a := 1 : N$ **do**
3: $\quad c_{T_a,E_{a-1}}^0 := \begin{cases} 0 & \text{if } a = 1, \\ ([G_h]_E \cdot \nu_E, \varphi_z)_{L^2(E_{a-1})} - c_{T_{a-1},E_{a-1}}^0 & \text{else} \end{cases}$
4: $\quad c_{T_a,E_a}^0 := (f + \operatorname{div} G_h, \varphi_z)_{L^2(T_a)} - c_{T_a,E_{a-1}}^0$
5: $\quad$ **for** $1 \leq \ell + m \leq q$ **do**
6: $\quad\quad c_{T_a,\mathrm{div}}^{\ell,m} := (f + \operatorname{div} G_h, \varphi_z x_1^\ell x_2^m)_{L^2(T_a)}$
7: $\quad$ **end for**
8: $\quad$ **for** $1 \leq j \leq q$ **do**
9: $\quad\quad c_{T_a,E_{a-1}}^j := 0$
10: $\quad\quad c_{T_a,E_a}^j := ([G_h]_E \cdot \nu_E, \varphi_z s^j)_{L^2(E_a)}$
11: $\quad$ **end for**
12: **end forOutput:** $\tilde{\sigma}_z^\Delta \in RT_q^{\mathrm{pw}}(\mathcal{T}(z))$ defined by (73) with coefficients $c_{T,E}^j$, $c_{T,\mathrm{div}}^{\ell,m}$, c_T^r.

This subsection presents the equilibration procedure, starting with Algorithm 2, that computes an admissible function $\tilde{\sigma}_z^\Delta \in \mathcal{S}(z)$ in terms of the representation (73). Enumerate the $N := |\mathcal{T}(z)|$ triangles $T \in \mathcal{T}(z)$ from 1 to N as in Fig. 7. Any two neighbouring triangles T_a, T_{a+1} share an edge $E_a := T_a \cap T_{a+1}$ for $a = 1, ..., N-1$. If $z \in \mathcal{V}(\Omega)$ is an interior vertex, T_1 and T_N share an additional edge $E_0 := E_N := T_1 \cap T_N$. For a boundary vertex $z \in \mathcal{V}(\partial\Omega)$, T_1, T_N have the distinct boundary edges $E_0, E_N \in \mathcal{F}(z) \cap \mathcal{F}(\partial\Omega)$. The following lemma shows correctness of Algorithm 2 under the compatibility condition (5) and represents step one of the equilibration algorithm. The final step is the local minimization problem in Lemma 12 that provides $Q_{z,h}^\Delta$ from (69). Both proofs are provided in A.4.

Lemma 11 *Given $z \in \mathcal{V}$, let $\{\varphi_{T,E}^j, \varphi_{T,\mathrm{div}}^{\ell,m}, \varphi_T^r\}$ be the basis of $RT_q(T)$ dual to Λ_T with (72) for all $T \in \mathcal{T}(z)$. Suppose $f \in L^2(\omega(z))$ and $G_h \in P_q(\mathcal{T}(z); \mathbb{R}^2)$ satisfy*

$$(G_h, \nabla\varphi_z)_{L^2(\omega(z))} = (f, \varphi_z)_{L^2(\omega(z))} \quad \text{if } z \in \mathcal{V}(\Omega). \tag{75}$$

Then the output of Algorithm 2 with input f and G_h defines a function $\tilde{\sigma}_z^\Delta \in \mathcal{S}(z)$.

Note that (75) is a local version of (5) and therefore holds for the HHO method with the choice $G_h := \nabla_{\mathrm{pw}} R u_h$ as proven in (20). This allows for the computation of $Q_p^\Delta := \sum_{z\in\mathcal{V}} Q_{z,h}^\Delta = Q_p - G_h$ in terms of local and unconstrained minimization problems on the vertex-patches $\omega(z)$.

Lemma 12 *Given $z \in \mathcal{V}$, let $\{\varphi_{T,E}^j, \varphi_{T,\mathrm{div}}^{\ell,m}, \varphi_T^r\}$ be as in Lemma 11 for all $T \in \mathcal{T}(z)$ and let $\tilde\sigma_z^\Delta \in \mathcal{S}(z)$ be arbitrary. Then $V(z) := \mathcal{S}(z) - \tilde\sigma_z^\Delta$ is a linear vector space and consists of all functions of the form*

$$\sum_{a=1}^{N}\left(d_0(\varphi^0_{T_a,E_{a-1}} - \varphi^0_{T_a,E_a}) + \sum_{\ell=1}^{q}(d^\ell_{E_{a-1}}\varphi^\ell_{T_a,E_{a-1}} - d^\ell_{E_a}\varphi^\ell_{T_a,F_a}) + \sum_{r=1}^{N_q} d^r_{T_a}\varphi^r_{T_a}\right) \tag{76}$$

for arbitrary $d_0, d^\ell_{E_a}, d^r_{T_a} \in \mathbb{R}$ with $\ell = 1, ..., q, r = 1, ..., N_q, a = 1, ..., N$ (and $d^\ell_{E_0} = d^\ell_{E_N}$ for $z \in \mathcal{V}(\Omega)$) and the enumeration of $\mathcal{T}(z)$ as in Fig. 7. Furthermore, $Q_{z,h}^\Delta = \tilde\sigma_z^\Delta + \sigma_z^\Delta$ holds for the solution $\sigma_z^\Delta \in V(z)$ to the $1+q|\mathcal{F}(z)|+q(q-1)/2N$-dimensional minimization problem (71).

A. 4 Proofs

The remaining parts of this appendix are devoted to the verification of Lemmas 11–12.

Proof (of Lemma 11) Enumerate $\mathcal{T}(z)$ as in A.3 and recall the definition of the jump $[G_h]_E = G_h|_{T_+} - G_h|_{T_-}$ on the interior edge $E = T_+ \cap T_-$ shared by $T_+, T_- \in \mathcal{T}$, and $[G_h]_E = G_h|_{T_+}$ for the unique triangle $T_+ \in \mathcal{T}$ with $E \subset T_+$ for the boundary edge $E \in \mathcal{F}(\partial\Omega)$. First, observe that $\sigma_z \in RT_q^{\mathrm{pw}}(\mathcal{T}(z))$ lies in $RT_q^{\mathrm{pw},0}(\mathcal{T}(z))$ if and only if the coefficients $c^j_{T,E} = 0$ in the representation (73) are zero for $0 \le j \le q$ at the edge $E \in \mathcal{F}(T)\backslash\mathcal{F}(z)$ in $T \in \mathcal{T}$ opposing z. By definition, $\sigma_z \in RT_q^{\mathrm{pw},0}(\mathcal{T}(z))$ belongs to $\mathcal{S}(z)$ if and only if

$$\lambda^{\ell,m}_{T,\mathrm{div}}(\sigma_z) = (f + \operatorname{div} G_h, \varphi_z x_1^\ell x_2^m)_{L^2(T)} \quad \text{for all } 0 \le \ell + m \le q, T \in \mathcal{T}(z), \tag{77}$$

$$(\lambda^j_{T_+,E} + \lambda^j_{T_-,E})(\sigma_z) = ([G_h]_E \cdot \nu_E, \varphi_z s^j)_{L^2(E)} \quad \text{for all } 0 \le j \le q, E \in \mathcal{F}(\omega(z)). \tag{78}$$

This translates into equivalent conditions on the coefficients of σ_z in the representation (73), namely, for all $a = 1, ..., N$,

$$c^0_{T_a,E_a} = (f + \operatorname{div} G_h, \varphi_z)_{L^2(T_a)} - c^0_{T_a,E_{a-1}}, \tag{79}$$

$$c^{\ell,m}_{T_a,\mathrm{div}} = (f + \operatorname{div} G_h, \varphi_z x_1^\ell x_2^m)_{L^2(T_a)} \quad \text{for all } 1 \le \ell + m \le q, \tag{80}$$

$$c^j_{T_a,E_{a-1}} = d^j_{E_{a-1}} \quad \text{for all } 0 \le j \le q, \tag{81}$$

$$c^j_{T_a,E_a} = ([G_h]_E \cdot \nu_E, \varphi_z s^j)_{L^2(E_a)} - d^j_{E_a} \quad \text{for all } 0 \le j \le q, \tag{82}$$

where $d^\ell_{E_a} \in \mathbb{R}$. Since $\sigma_z \in RT^{\mathrm{pw},0}_q(\mathcal{T}(z))$ vanishes at the other edges $E \in \mathcal{F} \setminus \mathcal{F}(z)$, $\lambda^{0,0}_{T_a,\mathrm{div}}(\sigma_z) = c^0_{T_a,E_{a-1}} + c^0_{T_a,E_a}$ and (79)–(80) are equivalent to (77). The identification $d^\ell_{E_0} = d^\ell_{E_N}$ for an interior vertex $z \in \mathcal{V}(\Omega)$ with $E_0 = E_N \in \mathcal{F}(z)$ shows that (81)–(82) are equivalent to (78). This identification is well defined. Note that, whereas there is no condition on $d^\ell_{E_a}$ for $1 \le \ell \le q$, the combination of (79) and (81) with (82) shows the implicit extra condition

$$d^0_{E_a} = d^0_{E_0} + \sum_{\alpha=1}^{a} \big(([G_h]_E \cdot \nu_E, \varphi_z)_{L^2(E_\alpha)} - (f + \operatorname{div} G_h, \varphi_z)_{L^2(T_\alpha)} \big) \quad \text{for } a = 0, \ldots, N.$$

For an interior vertex $z \in \mathcal{V}(\Omega)$, an integration by parts and (75) show that the sum on the right-hand side above vanishes for $a = N$, whence $d^0_{E_N} = d^0_{E_0}$ is indeed well defined. Furthermore, there is no condition on the coefficients $c^r_{T_a}$ for all $T_a \in \mathcal{T}(z)$ and $r = 1, \ldots, N_q$ and $c^r_{T_a} = d^r_{T_a}$ is a further degree of freedom.

Algorithm 2 finds coefficients that satisfy (79)–(82) in a loop over $a = 1, \ldots, N$ and therefore defines $\tilde\sigma^\Delta_z \in \mathcal{S}(z)$ by (73). □

Proof (of Lemma 12) This follows immediately after revisiting the proof of Lemma 11 for an arbitrary function $\sigma_z \in RT^{\mathrm{pw},0}_q(\mathcal{T}(z))$. Since $\sigma_z \in \mathcal{S}(z)$ is equivalent to (79)–(82) for the representation (73) of σ_z in the given basis, all functions $\sigma_z \in \mathcal{S}(z) - \tilde\sigma^\Delta_z$ are of the form (76) for arbitrary $d_0, d^\ell_{E_a}, d^r_{T_a} \in \mathbb{R}$ with $\ell = 1, \ldots, q$, $r = 1, \ldots, N_q$, and $a = 1, \ldots, N$ (and $d^\ell_{E_0} = d^\ell_{E_N}$ for $z \in \mathcal{V}(\Omega)$). Hence, the dimension of the linear space $V(z) = \mathcal{S}(z) - \tilde\sigma^\Delta_z$ is $1 + q|\mathcal{F}(z)| + q(q-1)/2N$. The claim follows from Proposition 1 by observing

$$Q^\Delta_{z,h} := \operatorname*{arg\,min}_{\sigma_z \in \mathcal{S}(z)} \|\sigma_z\|_{L^2(\omega(z))} = \tilde\sigma^\Delta_z + \operatorname*{arg\,min}_{\sigma_z \in \mathcal{S}(z) - \tilde\sigma^\Delta_z} \|\tilde\sigma^\Delta_z + \sigma_z\|_{L^2(\omega(z))}. \quad \square$$

□

References

1. Ainsworth, M.: Robust a posteriori error estimation for nonconforming finite element approximation. SIAM J. Numer. Anal. **42**(6), 2320–2341 (2005)
2. Ainsworth, M.: A posteriori error estimation for lowest order Raviart–Thomas mixed finite elements. SIAM J. Sci. Comput. **30**, 189–204 (2007)
3. Ainsworth, M., Oden, J.T.: A unified approach to a posteriori error estimation using element residual methods. Numer. Math. **65**, 23–50 (1993)
4. Alonso, A.: Error estimators for a mixed method. Numer. Math. **74**(4), 385–395 (1996)
5. Bertrand, F., Boffi, D.: The Prager-Synge theorem in reconstruction based a posteriori error estimation. In: 75 Years of Mathematics of Computation, vol. 754, pp. 45–67. Amer. Math. Soc., Providence, RI (2020)
6. Bertrand, F., Kober, B., Moldenhauer, M., Starke, G.: Weakly symmetric stress equilibration and a posteriori error estimation for linear elasticity. Numer. Methods Part. Differ. Equ. **37**(4), 2783–2802 (2021)
7. Boffi, D., Brezzi, F., Fortin, M.: Mixed Finite Element Methods and Applications, vol. 44. Springer, Heidelberg (2013)

8. Bonito, A., Nochetto, R.H.: Quasi-optimal convergence rate of an adaptive discontinuous Galerkin method. SIAM J. Numer. Anal. **48**(2), 734–771 (2010)
9. Braess, D.: Finite Elements: Theory, Fast Solvers, and Applications in Solid Mechanics, 3rd edn. Cambridge University Press, Cambridge (2007)
10. Braess, D., Pillwein, V., Schöberl, J.: Equilibrated residual error estimates are p-robust. Comput. Methods Appl. Mech. Eng. **198**, 1189–1197 (2009)
11. Brezzi, F., Fortin, M.: Mixed and Hybrid Finite Element Methods, vol. 15. Springer, New York (1991)
12. Cai, Z., Zhang, S.: Robust equilibrated residual error estimator for diffusion problems: conforming elements. SIAM J. Numer. Anal. **50**(1), 151–170 (2012)
13. Carstensen, C.: A posteriori error estimate for the mixed finite element method. Math. Comput. **66**(218), 465–476 (1997)
14. Carstensen, C.: A unifying theory of a posteriori finite element error control. Numer. Math. **100**(4), 617–637 (2005)
15. Carstensen, C., Ern, A., Puttkammer, S.: Guaranteed lower bounds on eigenvalues of elliptic operators with a hybrid high-order method. Numer. Math. **149**(2), 273–304 (2021)
16. Carstensen, C., Feischl, M., Page, M., Praetorius, D.: Axioms of adaptivity. Comput. Math. Appl. **67**(6), 1195–1253 (2014)
17. Carstensen, C., Gedicke, J., Rim, D.: Explicit error estimates for Courant, Crouzeix–Raviart and Raviart–Thomas finite element methods. J. Comput. Math. **30**(4), 337–353 (2012)
18. Carstensen, C., Gudi, T., Jensen, M.: A unifying theory of a posteriori error control for discontinuous Galerkin FEM. Numer. Math. **112**(3), 363–379 (2009)
19. Carstensen, C., Hellwig, F.: Constants in discrete Poincaré and Friedrichs inequalities and discrete quasi-interpolation. Comput. Methods Appl. Math. **18**(3), 433–450 (2018)
20. Carstensen, C., Hu, J.: A unifying theory of a posteriori error control for nonconforming finite element methods. Numer. Math. **107**(3), 473–502 (2007)
21. Carstensen, C., Peterseim, D., Schröder, A.: The norm of a discretized gradient in $H(\mathrm{div})^*$ for a posteriori finite element error analysis. Numer. Math. **132**, 519–539 (2016)
22. Carstensen, C., Rabus, H.: Axioms of adaptivity with separate marking for data resolution. SIAM J. Numer. Anal. **55**(6), 2644–2665 (2017)
23. Ciarlet, P., Dunkl, C.F., Sauter, S.A.: A family of Crouzeix–Raviart finite elements in 3D. Anal. Appl. (Singap.) **16**(5), 649–691 (2018)
24. Dauge, M.: Elliptic Boundary Value Problems on Corner Domains, vol. 1341. Springer, Berlin (1988)
25. Di Pietro, D.A., Droniou, J.: The Hybrid High-Order Method for Polytopal Meshes, vol. 19. Springer, Cham (2020)
26. Di Pietro, D.A., Ern, A.: A hybrid high-order locking-free method for linear elasticity on general meshes. Comput. Methods Appl. Mech. Engrg. **283**, 1–21 (2015)
27. Di Pietro, D.A., Ern, A., Lemaire, S.: An arbitrary-order and compact-stencil discretization of diffusion on general meshes based on local reconstruction operators. Comput. Methods Appl. Math. **14**(4), 461–472 (2014)
28. Ern, A., Guermond, J.L.: Finite Elements I-Approximation and Interpolation, vol. 72. Springer, Cham (2021)
29. Ern, A., Guermond, J.L.: Finite Elements II–Galerkin Approximation, Elliptic and Mixed PDEs, vol. 73. Springer, Cham (2021)
30. Ern, A., Vohralík, M.: Polynomial-degree-robust a posteriori estimates in a unified setting for conforming, nonconforming, discontinuous Galerkin, and mixed discretizations. SIAM J. Numer. Anal. **53**(2), 1058–1081 (2015)
31. Ern, A., Vohralík, M.: Stable broken H^1 and $H(\mathrm{div})$ polynomial extensions for polynomial-degree-robust potential and flux reconstruction in three space dimensions. Math. Comput. **89**(322), 551–594 (2020)
32. Ern, A., Zanotti, P.: A quasi-optimal variant of the hybrid high-order method for elliptic partial differential equations with H^{-1} loads. IMA J. Numer. Anal. **40**(4), 2163–2188 (2020)
33. Girault, V., Raviart, P.A.: Finite Element Methods for Navier–Stokes Equations, vol. 5. Springer, New York (1986)
34. Kikuchi, F., Liu, X.: Estimation of interpolation error constants for the P_0 and P_1 triangular finite elements. Comput. Methods Appl. Mech. Eng. **196**(37–40), 3750–3758 (2007)
35. Oikawa, I.: A hybridized discontinuous Galerkin method with reduced stabilization. J. Sci. Comput. **65**(1), 327–340 (2015)

36. da Veiga, L.B., Canuto, C., Nochetto, R.H., Vacca, G., Verani, M.: Adaptive VEM: Stabilization-free a posteriori error analysis. SIAM J. Numer. Anal **61**(2), 457–494 (2023)
37. Verfürth, R.: A note on constant-free a posteriori error estimates. SIAM J. Numer. Anal. **47**(4), 3180–3194 (2009)
38. Verfürth, R.: A Posteriori Error Estimation Techniques for Finite Element Methods. Oxford University Press, Oxford (2013)
39. Wang, J., Ye, X.: A weak Galerkin finite element method for second-order elliptic problems. J. Comput. Appl. Math. **241**, 103–115 (2013)